the plant journal

Isolation and characterization of mutants corresponding to the MENA, MENB, MENC, and MENE enzymatic steps of 5'-monohydroxyphylloquinone biosynthesis in Chlamydomonas reinhardtii.

Journal:	*The Plant Journal*
Manuscript ID	Draft
Manuscript Type:	Original Article
Date Submitted by the Author:	n/a
Complete List of Authors:	Emonds-Alt, Barbara; University of Liege, Life Sciences, Genetics and Physiology of Microalgae Coosemans, Nadine; University of Liege, Life Sciences, Genetics and Physiology of Microalgae Gerards, Thomas; Universite de Liege, Life Sciences, Bioenergetics Remacle, Claire; University of Liege, Life Sciences, Genetics and Physiology of Microalgae Cardol, Pierre; University of Liege, Life Sciences, Genetics and Physiology of Microalgae
Key Words:	Phylloquinone, photosynthesis, anoxia, insertional mutagenesis, Chlamydomonas reinhardtii

TITLE

Isolation and characterization of mutants corresponding to the MENA, MENB, MENC, and MENE enzymatic steps of 5'-monohydroxyphylloquinone biosynthesis in *Chlamydomonas reinhardtii*.

AUTHORS

Barbara Emonds-Alt[a], Nadine Coosemans[a], Thomas Gerards[b], Claire Remacle[a], Pierre Cardol[a*]

[a]Department of Life Sciences, Genetics and Physiology of Microalgae, PhytoSYSTEMS, InBios, University of Liège, B–4000 Liège, Belgium

[b]Department of Life Sciences, Bioenergetics, PhytoSYSTEMS, InBios, University of Liège, B–4000 Liège, Belgium

[*]corresponding author e-mail: pierre.cardol@ulg.ac.be

CORRESPONDING AUTHOR DETAILS

Pierre Cardol. B22 Institute of Botany, Genetics and Physiology of Microalgae, Quartier Vallée 1, Chemin de la Vallée 4, 4000 Liège 1, Belgium. E-mail: pierre.cardol@ulg.ac.be, tel: +32 4 3663840.

EMAIL ADDRESSES OF ALL THE AUTHORS

Barbara Emonds-Alt: barbara.emonds-alt@doct.ulg.ac.be ; Nadine Coosemans : nadine.coosemans@ulg.ac.be ; Thomas Gerards: tgerards@ulg.ac.be ; Claire Remacle: c.remacle@ulg.ac.be ; Pierre Cardol; pierre.cardol@ulg.ac.be

RUNNING TITLE

Loss of phylloquinone in *Chlamydomonas*.

KEY WORDS

Chlamydomonas reinhardtii, Phylloquinone, insertional mutagenesis, anoxia, photosynthesis

TOTAL WORD COUNT: 7837 words

(1) SUMMARY (196 words)

Phylloquinone (PhQ) or Vitamin K_1 is an essential electron carrier (A_1) in photosystem I (PSI). In the green alga *Chlamydomonas reinhardtii*, which is a model organism for photosynthesis study, a detailed characterization of the pathway is missing with only one mutant deficient for MEND that has been analyzed. We took advantage of the fact that a double reduction of plastoquinone occurs in anoxia into the A_1 site in the *mend* mutant, interrupting photosynthetic electron transfer, to isolate four new phylloquinone-deficient mutants impaired in *MENA*, *MENB*, *MENC* (*PHYLLO*) and *MENE*. Compared to wild-type and complemented strains for *MENB* and *MENE*, the four *men* mutants grow slowly in low light and are sensitive to high light. When grown in low light, they show a reduced photosynthetic electron transfer due to a specific decrease of PSI. Upon exposure to high light for a few hours, PSI becomes almost completely inactive, which leads in turn to lack of phototrophic growth. Loss of PhQ also fully prevents reactivation of photosynthesis after dark anoxia acclimation. *In silico* analyses allowed us to propose a PhQ biosynthesis pathway in *Chlamydomonas* that involves eleven enzymatic steps from chorismate located in the chloroplast and in the peroxisome.

(2) SIGNIFICANCE STATEMENT (25 words)

Chlamydomonas phylloquinone-deficient mutants impaired in MENA, -B, -C, and -E activities are light-sensitive, primarily affected in photosystem I, and unable to initiate photosynthesis in anoxia.

(3) INTRODUCTION (1058 words)

In cyanobacteria, algae and land plants, photosynthetic electron transfer is driven by two large intrinsic protein complexes, photosystem I (PSI) and photosystem II (PSII) embedded in the thylakoid membrane. Each PS possesses several cofactors, including quinones (benzoquinone or naphthoquinone derivatives) required for electron transfer. Plastoquinones (PQ) are benzoquinone derivatives (PQ) located in PSII (two binding sites, Q_A and Q_B) and in the PQ pool. PQ is doubly reduced into plastoquinol (PQH_2) at Q_B site and diffuses in the membrane to join PQ pool allowing then the reduction of cytochrome b_6f complex (cyt b_6f) (Rochaix, 2002). In contrast, naphthoquinone derivatives participate to electron transfer within PSI. PSI is composed of two core subunits, PsaA and PsaB, containing 11 transmembrane domains and forming the heterodimeric reaction center that coordinate cofactors required for electron transfer (Rochaix, 2002). The primary PSI electron donor is a dimer of chlorophyll a (P_{700}) located on the luminal side of the membrane. Electron transfer from P_{700} to ferredoxin occurs via chlorophyll A_0, naphthoquinone A_1 and three iron-sulfur centers [4Fe-4S] noted F_X, F_A and F_B. Two naphthoquinones are present by P_{700} and allow electron transfer from A_0 to F_X by two branches (A and B) (Joliot and Joliot, 1999; Guergova-Kuras et al., 2001). To date three types of 2-methyl-1,4-naphthoquinone derivatives, also known as vitamin K, have been identified in different oxygenic photosynthetic organisms. They share the same naphthalene nucleus but differ in the prenyl side-chain attached in position 3: menaquinone-4 (MK-4, vitamin K_2) found in bacteria, diatoms and red algae (Yoshida et al., 2003; Ikeda et al., 2008) has a fully unsaturated C_{20} isoprenoid side-chain; phylloquinone (PhQ, vitamin K_1) found in most cyanobacteria, green algae and land plants, has a phytyl side-chain (partially saturated C_{20} prenyl) while 5'monohydroxyphylloquinone (OH-PhQ) is found in *Euglena gracilis* and in some cyanobacteria like *Synechococcus elongatus* (Law et al., 1973; Omata and Murata, 1984). Some species such as the green microalga *Chlamydomonas reinhardtii* possess two types of naphthoquinones: PhQ and OH-PhQ (Ozawa et al., 2012). In *C. reinhardtii*, PhQ and OH-PhQ account for 10 and 90% of the total naphthoquinone content, respectively. Both are functional and contribute to the photosynthetic electron transfer (Ozawa et al., 2012).

The conversion of chorismate to menaquinone has been characterized in details in bacteria over the past decade (Meganathan, 2001; Jiang et al., 2007; Jiang et al., 2008; Chen et al., 2013). Since the different types of naphthoquinones are structurally close, most of the components of the phylloquinone biosynthesis pathway in the cyanobacteria *Synechocystis* sp. PCC 6803 have been identified by searching the cyanobacterial genome using bacterial genes as queries. In *Synechocystis*, nine enzymes, characterized by reverse genetics, catalyze the same steps as those required for synthesis of menaquinone: MenF (isochorismate synthase), MenD (2-succinyl-5-enolpyruvyl-6-hydroxy-3-cyclohexene-1-carboxylic acid (SEPHCHC) synthase), MenH (2-succinyl-6-hydroxy-2,4-cyclohexadiene-1-carboxylate (SHCHC) synthase), MenC (*o*-succinylbenzoic acid synthase), MenE (*o*-succinylbenzoyl-CoA ligase), MenB (1,4-dihydroxy-2-naphtoate (DHNA) synthase), Slr0204 (1,4-dihydroxy-2-naphthoate (DHNA)-CoA thioesterase), MenA (DHNA phytyltransferase), and MenG (methyltransferase) (Johnson et al., 2000; Johnson et al., 2001; Widhalm et al., 2009) (Table 1).

In *Synechocystis*, inactivation of *menA*, *–B*, *–D* and *–E* genes leads to the complete absence of phylloquinone, which is replaced by PQ in the A_1 site of PSI (Johnson et al., 2000; Semenov et al., 2000; Johnson et al., 2001; Johnson et al., 2003). This substitution leads to a delayed electron transfer from A_1^- to F_X because the redox potential of PQ in the A_1 site is more oxidizing than native PhQ, rendering the electron transfer thermodynamically unfavorable. These mutants grow slowly under low light conditions and are sensitive to high light. In contrast, inactivation of *menG*, the last enzyme of the phylloquinone biosynthetic pathway, results in the accumulation of demethylphylloquinone which replaces PhQ in PSI (Sakuragi et al., 2002). The *menG* mutant is characterized by a normal growth although electron transfer from A_1^- to F_X is three times slower. All *Synechocystis men* mutants are characterized by a decreased PSI/PSII ratio but only under high light for *menG*.

Mutants deficient in PhQ biosynthesis pathway have also been identified in photosynthetic eukaryotes. In *Arabidopsis thaliana*, inactivation of *ABC4* (*menA* homolog) leads to a significant decrease of PSII and PSI content, and PQ level is reduced to 3% (Shimada et al., 2005). Mutants in *PHYLLO* gene (which encodes a fusion of four eubacterial *men*-homologous regions corresponding to

menF/*menD*/*menC*/*menH* genes) have drastically reduced PSI levels (5-15%) with nearly normal levels of PSII and accumulate 55% of PQ (Gross et al., 2006). Mutants deleted for the *AAE14* gene (*menE* homolog), *ABC4* and *PHYLLO*, exhibits a seedling-lethal phenotype (Kim, 2008). In contrast, *Arabidopsis menG*-homologous deficient mutant is viable because, like in *Synechocystis*, demethylphylloquinone acts as PhQ substitute in PSI (Lohmann et al., 2006). Last year, it was established in *Synechocystis* and *Arabidopsis* that the biosynthesis of phylloquinone has an additional step : the reduction of the demethylphylloquinone ring by a type-II NADPH dehydrogenase named NdbB in *Synechocystis* and NDC1 in *Arabidopsis* prior to its transmethylation by MenG (Fatihi et al., 2015). *Synechocystis ndbB* and *Arabidopsis ndc1* mutants display increased photosensitivity to high light like phylloquinone-deficient mutants previously characterized in these organisms.

In the green alga *C. reinhardtii*, which is a model organism for the study of the photosynthetic machinery (Hippler et al., 1998), characterization of PhQ biosynthetic pathway is still partial. Up to now, only one mutant, deficient for MEND protein was characterized (Lefebvre-Legendre et al., 2007). Inactivation of *MEND* in *C. reinhardtii*, like in *Synechocystis* sp. PCC 6803 (Johnson et al., 2003), leads to the complete loss of PhQ and its replacement by PQ in PSI. However, accumulation of PSI is not affected in this mutant and the absence of PhQ rather causes a decrease in the size of the plastoquinone pool and of synthesis of PSII subunits.

The phenotype of the only mutant isolated in *C. reinhardtii* is thus neither closed to the one described in cyanobacteria neither to the one of land plants. This observation prompted us to isolate new mutants of the phylloquinone biosynthetic pathway in *C. reinhardtii.* In anoxia, a double reduction of PQ into PQH_2 in the A_1 site occurs in the *mend* mutant interrupting photosynthetic electron transfer (Lefebvre-Legendre et al., 2007; McConnell et al., 2011). In this work, we took advantage of this photosynthetic deficiency in anoxia to isolate four new *Chlamydomonas* mutants affected in one of the enzymatic steps of phylloquinone biosynthesis pathway (MENA, MENB, MENC and MENE).

(4) RESULTS (2298 words)

A peculiar chlorophyll induction curve is specific for identification of phylloquinone-deficient mutants

In *C. reinhardtii* genomic database (v5.5 on Phytozome), nine sequences corresponding to nine of the ten enzymatic steps required for phylloquinone biosynthesis pathway in cyanobacteria and land plants were found (Table 1). Genomic sequences coding for MENF, MEND, MENC and MENH enzymatic domains are located in a single ORF, named *PHYLLO* by similarity to gene organization in *Arabidopsis thaliana* (Gross et al., 2006), and likely coding for a tetramodular enzyme. We did not find any homolog to the DHNA-CoA thioesterase performing the seventh step of the pathway in cyanobacteria and land plants but a putative candidate (TEH4) is suggested (see discussion).

To isolate new strains deficient in phylloquinone biosynthesis in *C. reinhardtii*, we screened 13,250 hygromycin-resistant (Hyg^R) transformants and 3,500 paromomycin-resistant (Par^R) transformants by an *in vivo* chlorophyll fluorescence imaging screening protocol. The screening procedure is based on the observation that a double reduction of PQ in PQH_2 into the A_1 site occurs in a *mend* mutant in anoxia interrupting photosynthetic electron transfer (McConnell et al., 2011). We thus recorded chlorophyll fluorescence induction curves of transformants after prolonged dark anoxic incubation. As previously described (Godaux et al., 2013), for dark anoxic acclimated wild-type cells, F_O is close to F_M which indicated that the PSII acceptor pool (Q_a, PQ) is largely reduced. Upon illumination, the fluorescence yield reaches a maximal transient value in a few ms and then it decreases to a steady-state value after ~1 s. The value of the photosystem II efficiency (ΦPSII), determined after 3 s of illumination by addition of a saturating pulse reached 0.5 (Figure 1a). Conversely, the electron transfer was blocked from the very beginning of illumination in *mend* mutant and ΦPSII after 3 s of illumination is null (Figure 1a). We isolated here five Hyg^R (AL2, AO1, AO2, AS1, AS2) and two $Paro^R$ mutants (24.1, 25.1) with a similar chlorophyll fluorescence induction curve to *mend* (Figure 1b). In contrast, the behaviour of these mutants is

almost identical to wild type in control conditions (oxic) (Figure 1c). This suggested that these mutants were specifically impaired in phylloquinone biosynthesis.

To determine whether the fluorescence phenotype of these mutants was linked to the antibiotic-resistance cassette, a genetic cross between each mutant of mating-type plus (mt^+) was performed with wild-type strain of the opposite mating type (mt^-) and phenotype of the meiotic progeny was analyzed (Table S1). For four mutants (AO1, AS1, AS2 and 25.1) all meiotic products that were resistant to antibiotic also showed mutant fluorescence phenotype, while all meiotic products that were sensitive to the presence of antibiotics behaved like wild type. In addition, around half of the meiotic progeny was resistant to antibiotics in each of the four crosses. This suggested that a unique functional cassette was linked to the phenotype of each individual mutant. In contrast, the presence of four classes of meiotic products in the progeny of AL2, AO2, and 24.1 indicated that the fluorescence phenotype was not directly linked to the insertion of the cassettes. As a consequence, these mutants (AL2, AO2 and 24.1) were discarded. To confirm that only one cassette was inserted in the genome of AO1, AS1, AS2 and 25.1 mutants, DNA gel-blot analysis was carried out on the four tagged mutant strains with specific probes against *APHVII* (for AO1, AS1 and AS2 mutants) and *APHVIII* (for 25.1 mutant) cassettes. As only one fragment was revealed after hybridization, we concluded that each mutant contained a single copy of the resistance cassette in its nuclear genome (Figure 2a). To determine genomic DNA sequences flanking the insertion cassette for each individual mutant, we performed thermal asymmetric interlaced (TAIL) PCR and the resulting PCR products were sequenced (Figure S1). A detailed description of this analysis is given in Appendix S1 and summarized in Figure 2b. In brief, the four mutants are all affected in one of the genes of the putative phylloquinone biosynthetic pathway in *Chlamydomonas*: *MENA* (AS2, *mena* mutant), *MENB* (AS1, *menb* mutant), *PHYLLO* (AO1, *menc* mutant) and *MENE* (25.1, *mene* mutant).

We then aimed at obtaining complemented strains as an additional proof of phenotype. To this end, we amplified *MENB* (4,865 bp) and *MENE* (4,177 bp) genes and their flanking regions (Figure S2). We could not however amplify *MENA* (3,136 bp).

Concerning *PHYLLO* (15.7 kb), we did not try to amplify the corresponding gene because it was too long to be amplified by PCR. *menb* cells and *mene* cells were then co-transformed using the appropriate selection marker (*APHVIII* and *APHVII*, respectively) and the PCR product containing *MENB* or *MENE* gene, respectively. Transformants were selected on medium containing both hygromycin and paromomycin and co-transformants which have incorporated and expressed the second marker (either *MENB* or *MENE*) were selected on the basis of their restored wild-type fluorescence pattern after acclimation to dark anoxic conditions (Figure S3). One complemented co-transformant was selected for each strain, and called *menbR* and *meneR,* respectively.

Absence of phylloquinone in the *men* mutant strains

To determine the impact of *mena*, *menb*, *menc* and *mene* mutations on phylloquinone abundance, pigments were extracted from lyophilized cells and analysed by UPLC-MS. The elution profile of the *men* mutant cell extracts was compared with those of wild-type and complemented cell extracts. Because about 90% of the total amount of naphthoquinones in *C. reinhardtii* is present as OH-PhQ (Ozawa et al., 2012), we decided to focus on the detection of this form. OH-PhQ whose determined m/z values of non-adduct form and Na^+ adduct form are respectively 467.35 and 489.33, was detected as a single peak at 8.06 min of the chromatogram of wild-type and complemented cell extracts. This peak was missing in the *men* mutant cell extracts (Figure 3) indicating loss of OH-PhQ.

Light response of phylloquinone-deficient mutants

Since the previously isolated *Chlamydomonas mend* mutant is light sensitive (Lefebvre-Legendre et al., 2007), we analyzed the growth of *mena*, *menb*, *menc*, *mend* and *mene* mutant strains in the presence (TAP medium) or in the absence (TMP medium) of acetate. We emphasized on comparing growth at low and high light intensities for mutant and control strains. After 3 days of illumination, all mutants grew more slowly than wild-type and complemented strains, whatever the medium and the light conditions used (Figure 4). At day 7, this delayed growth is not observed anymore on acetate

medium (TAP) in the dark and under low light (25 µmol photons m^{-2} s^{-1}) but is still visible in the other conditions, *e. g.* under higher light (125 and 300 µmol photons m^{-2} s^{-1}) in the presence (TAP) or in the absence (TMP) of acetate in the medium. In addition, it has been shown that growth of *mend* could be partially restored by addition of exogenous phylloquinone at high light intensities (Lefebvre-Legendre et al., 2007). This was also the case for *menb*, *menc* and *mene* mutants, suggesting that the three mutants are auxotrophic for PhQ. In contrast, the addition of exogenous PhQ had no effect on the growth of *mena* mutant (Figure 4).

Reorganization of the photosynthetic apparatus in the absence of phylloquinone

In order to investigate the impact of the lack of phylloquinone on photosynthesis, we first determined the content of active PSI and PSII in mutant and control strains by a spectroscopic approach based on the magnitude of the electrochromic shift (ECS) induced by a charge separation (Bailleul et al., 2010). We observed a decrease of 30-40% of active PSI centers in all mutant strains (Figure 5a). This decrease in active PSI content was further confirmed by assessing the relative concentration of P_{700} by redox difference spectroscopy (Figure S4) and by immunoblotting on western blot against PsaA protein (Figure 5c). Similarly, in line with previous immunoblotting experiments against PSII core proteins D1 and D2 (Lefebvre-Legendre et al., 2007), the amount of active PSII (Figure 5a) and core antenna subunit Cp43 (Figure 5c) was very low in the *mend* mutant. Conversely, no decline in PSII centers was observed in the four *men* mutants identified in this work (Figure 5a and Figure 5c).

To gain information on excitation energy distribution between PSI and PSII, we also recorded 77K fluorescence emission spectra of whole *C. reinhardtii* cells. Excitation in the Chlorophyll Soret band produces PSII and PSI fluorescence bands at 685 and 715 nm, respectively, each band resulting from fluorescence emission of different forms of PS-LHC supercomplexes [*e.g.* ranging from 708 to 715 nm in the case of PSI (Drop et al., 2011)]. In *men* mutant cells frozen to 77 K under the white low light used for growth, the relative amplitude of 715 nm peak was larger than in wild-type and complemented strains (Figure 5g). This result suggests a relative increase in PSI

antenna size in *men* mutant cells due to (i) a larger light-harvesting complexes I (LHCI) or (ii) an association of LHCII to PSI (*i.e.* a transition to state II due to a more reduced state of the plastoquinone (PQ) pool (Wollman, 2001). To test these hypotheses, we treated the cells with DCMU to inhibit PSII and to reoxidize the PQ pool in the light, thus allowing association of LHCII back to PSII (*i.e.* transition to state 1) (Cardol et al., 2003). In wild-type and complemented strains, this treatment leads to a full transition to state 1, detected as a decrease of the relative amplitude of the 715 nm band. In contrast, DCMU-treated *men* cells still show a higher emission at 715nm relative to 685 nm. To confirm this result, we measured PSI antenna size at state I using ECS (Bailleul et al., 2010; Takahashi et al., 2013). The initial slope of the ECS changes measured in continuous light and in the presence of DCMU (to inhibit PSII) can be used to probe the absorption cross-section of PSI because it is proportional to the light intensity (Figure S5a). An increase in PSI antenna size was observed in all *men* mutants compared to controls strains (20-50 % increase) (Figure 5h). In parallel, PSII antenna size was estimated from mid-rise values of the chlorophyll fluorescence transients measured in continuous light and in the presence of DCMU at state 1 (Figure S5b). PSII antenna size remained unchanged, at the exception of *mend* (70 % increase) (Figure 5h).

We finally explored the impact of the imbalance in PSI/PSII stoichiometry and antenna size of *men* mutants on the relative electron transfer rate at PSII level ($rETR_{II}$). When cultivated in low light, *men* mutants exhibited a significant decrease of $rETR_{II}$ compared to wild-type and complemented strains (Figure 5e). A decrease of ~ 30% is observed for *mena* and *menb* mutants and of ~ 60% for *menc*, *mend* and *mene* mutants.

So far all spectroscopic experiments were carried out on algae grown under low light. In these conditions, *men* mutants are still able to grow (Figure 4) even if a decrease in the number of active PSI centers limits the photosynthetic electron flow. In contrast mutants are unable to grow under high light. We thus assumed the existence of additional deleterious effects on the photosynthetic chain in algal cells under high light. To test this hypothesis, wild-type and mutants cells were grown in low light (25 µmol photons m^{-2} s^{-1}) and then transferred for four hours at high light intensity (400 µmol photons m^{-2} s^{-1}). After 4 hours in high light, the content of active PSI centers remained relatively

constant in WT and complemented strains, but it progressively decreased over time in *mena*, *menb*, *menc* and *mene* to less than 10% of controls and in *mend* by half (Figure 5b and S6). Conversely, the amount of active PSII centers already fell at a steady level after one hour in high light in control strains (40-60% decrease) and *men* mutants (70-80% decrease) (Figures 5b and S6), indicating a more pronounced PSII photoinhibition in all *men* strains. Consistently, $rETR_{II}$ was drastically reduced in all *men* strains after four hours under high light (~ 20% of the wild-type) (Figure 5f).

To determine whether the decrease in the number of active PS is associated with a decrease in the total amount of PS per cell, or a loss of activity of PS centers present after exposure to high light (4 hours), the amount of core subunit PsaA (PSI) and core antenna subunit Cp43 (PSII) were compared to the amount of cytochrome *f* (cytochrome b_6f complex) by immunodetection on western blot on total cell extracts (Figure 5d). PsaA content was lower in all *men* mutants but this decrease was not especially more pronounced in comparison to the decrease in the amount of PsaA observed for low light-adapted *men* mutant cells. We concluded that the decrease of $rETR_{II}$ in *men* mutant exposed to high light is thus due to a specific PSI photoinhibition.

It is to note that *mend* mutant behaves slightly differently. Its PSII content is much lower in low light (Figures 5a and 5c), which is in agreement with its original description (Lefebvre-Legendre et al., 2007). Upon exposure to high light, this reduced PSII content might limit electron flow to PSI which translates into a lower PSI photoinhibition compared to other *men* mutants (Figure 5b). In principle both *menc* and *mend* mutants should be affected in the whole *PHYLLO* locus and thus should behave exactly the same. As a matter of proof, a RT-PCR experiment indicated that the mRNA segment corresponding to MENC-MENH domain is absent in *mend* mutant, as in *menc* mutant (Figure S7). We tried to determine if a secondary mutation could be responsible of the partly rescued phenotype of *mend* but unfortunately it was impossible to cross *mend* with our wild-type reference strains. We postulate that *mend* mutant (Lefebvre-Legendre et al., 2007) has been subject to adaptations that led to the observed decrease in PSII content and consequently to a lower PSI photoinhibition (Figures 5a, 5b and S6), and a better growth (Figure 4).

(5) DISCUSSION (1850 words)

Phylloquinone biosynthesis pathway might comprise eleven enzymatic steps located in the chloroplast and in the peroxisome

C. reinhardtii genomic data (Table 1) indicate that the biosynthesis pathway of phylloquinone (PhQ) from chorismate comprises homologs for nine of the ten consecutive enzymatic steps involved in PhQ biosynthesis in *Synechocystis sp*. PCC 6803 and in *Arabidopsis thaliana* (Fatihi et al., 2015). We did not find any obvious homolog of the cyanobacterial and plant DHNA-CoA thioesterase nor in *Chlamydomonas* neither in other green algae (*e.g. Chlorella vulgaris* C-169, *Chlorella sp*. NC64A, *Volvox carteri*). It is to note that the plant and cyanobacteria DHNA-CoA thioesterases are not encoded by homologous genes, the plant version originating from a horizontal gene transfer with a bacterial species (Widhalm et al., 2012). Altogether, this suggests that another thioesterase might operate in PhQ biosynthesis pathway of green algae. Among the large family of thioesterases in *Chlamydomonas reinhardtii*, TEH4 (Cre07.g323150) is a possible candidate because it possesses the hot-dog domain typical of DHNA-CoA thioesterase (Furt et al., 2013), a putative binding site for Co-enzyme A, and a peroxisomal targeting sequence (PTS) (see below for further discussion). In flowering plants, genetic approaches identified the *PHYLLO* locus which codes for a multienzyme composed of four fused eubacterial *men*-homologous modules corresponding to MenF/MenD/MenC/MenH proteins, respectively (Gross et al., 2006). Homology searches revealed the existence of cluster *PHYLLO* orthologues in green algae, mosses, diatoms and red algae (Gross et al., 2006). The C-terminal region bearing the chorismate binding site is absent from PHYLLO MENF module in *Arabidopsis*, and isochorismate synthase (ICS) activity is performed by *ICS1* and *ICS2* gene products (Gross et al., 2006; Garcion et al., 2008). PHYLLO then catalyzes consecutive reactions (MEND, C, and H) that lead to the synthesis of *o*-succynilbenzoate (Gross et al., 2006). In contrast to *Arabidopsis* PHYLLO protein, *C.*

reinhardtii nuclear genome likely encodes a PHYLLO tetramodular enzyme that would exhibit a full MENF chorismate binding domain that might be functional (Figure 2b and S8). Accordingly, we thus assume that our *Chlamydomonas* mutants are impaired in the fourth (MENC), the fifth (MENE), the sixth (MENB), and the eighth (MENA) enzymatic steps of PhQ biosynthesis (Figure 7). The previously characterized *mend* mutant (Lefebvre-Legendre et al., 2007) would be impaired in the second step. Even if the existence of a tetramodular PHYLLO enzyme remains to be demonstrated beyond genomic evidences, it is however reasonable to consider at this stage that *menc* and *mend* mutants are impaired in the function of the whole PHYLLO multienzyme (*i.e.* including MENF and MENH activities).

Ultimately, four steps remain to be characterized by genetic approaches in *Chlamydomonas*: the step 7 is the putative DHNA-CoA thioesterase TEH4; the step 9 would be performed by the type II NADPH dehydrogenase NDA5 which is the homolog of *Arabidopsis* NDC1 and *Synechocystis* NdbB (Desplats et al., 2009); step 10 is probably performed by the MENG homolog, and an ultimate additional step (step 11) of hydroxylation of PhQ to OH-PhQ, specific to some microalgae like *Chlamydomonas reinhardtii* and *Euglena gracilis* (Ziegler et al., 1989; Ozawa et al., 2012) remains also to be elucidated. In this regard, two Cytochrome P450-dependent PhQ hydroxylase have been recently identified (CYP4F2 and CYP4F11) in human (Edson et al., 2013). A putative homolog (CYP25, Cre08.g373100) is present in *Chlamydomonas* (Figure S9) and could fulfill the role.

Localisation of the phylloquinone biosynthesis pathway in *Chlamydomonas* is also unknown. Mainly originating from the cyanobacterial ancestor, most of the proteins involved in biosynthesis of PhQ in *Arabidopsis* are located in chloroplast (Shimada et al., 2005; Gross et al., 2006; Lohmann et al., 2006; Garcion et al., 2008; Kim, 2008). MenE/AAE14 has however a dual localization in chloroplast and peroxisome (Kim, 2008; Babujee et al., 2010), while MenB/NS and DHNA-CoA thioesterases are targeted to the peroxisome (Reumann et al., 2007; Babujee et al., 2010) (Widhalm et al., 2012). Here we took advantage of the recent identification of PTS motifs in *C. reinhardtii*, which are similar to *Arabidopsis* PTS (Lauersen et al., 2016), to identify three PTS sequences among *Chlamydomonas* peptide sequences discussed in this work : a PTS1

(SRL) in MENE and TEH4 C-terminal parts (position 732-734 and 201-203, respectively), and a PTS2 in MENB N-terminal part (RLqvlsnHL at position 7-15). This suggests that in *Chlamydomonas* like in *Arabidopsis*, this part of the biosynthetic pathway also occurs in the peroxisome but this hypothesis remains to be confirmed by subcellular localisation experiments. Altogether, our results suggest that localization of the steps involved in PhQ biosynthesis pathway in *Chlamydomonas* (Figure 7) might be very similar to the one previously described in land plants (Fatihi et al., 2015), and that there is no alternative route for PhQ synthesis in *Chlamydomonas*. We thus propose that chorismate is converted into *o*-succinylbenzoate by the first four enzymatic steps (PHYLLO) in the chloroplast. Then, *o*-succinylbenzoate would be exported to the peroxisome where the succinyl chain would be activated by ligation with CoA and cyclised to yield 1,4-dihydroxy-2-naphtoyl(DHNA)-CoA. After DHNA-CoA hydrolysis by an unknown thioesterase possibly located in the peroxisome, the naphthoquinone ring would be conjugated to a phytyl chain. At last, demethylphylloquinone precursor would be reduced in demethylphylloquinol form, methylated into PhQ, and hydroxylated into OH-PhQ in the chloroplast (Figure 7).

Lack of phylloquinone primarily affects PSI activity

Phylloquinone (or Vitamin K_1) is an essential electron carrier in PSI. As previously demonstrated in *Chlamydomonas* and *Synechocystis*, plastoquinone (PQ) might replace the missing phylloquinone in the A_1 site of PSI, rendering the electron transfer from A_1^- to F_X thermodynamically unfavourable (Semenov et al., 2000; Lefebvre-Legendre et al., 2007; McConnell et al., 2011). In this work, we identified and characterized four new *C. reinhardtii* nuclear insertion mutants deficient for 5'-monohydroxyphylloquinone (OH-PhQ), the predominant form of naphthoquinone in this species (Ozawa et al., 2012). All *Chlamydomonas men* mutants [including *mend* previously characterized (Lefebvre-Legendre et al., 2007)] can grow photoautotrophically under moderate light (25 µmol photons m^{-2} s^{-1}) but are high light-sensitive. *Arabidopsis abc4* (MENA), *phyllo* (PHYLLO MENDCH), *aae14* (MENE) and double knockout *ics1*/*ics2* (MENF) mutants are also characterized by loss of phototrophy and seedling lethal phenotype even in low light but it is not known if missing PhQ is replaced by PQ in this species (Shimada et

al., 2005; Gross et al., 2006; Garcion et al., 2008; Kim, 2008). The *Arabidopsis* MENG and NDC1 mutants are the sole viable PhQ-deficient mutants in plants (Lohmann et al., 2006; Fatihi et al., 2015). *Synechocystis* and *Arabidopsis meng* and *ndc1* mutants accumulate demethylphylloquinone which replaces PhQ and allows less efficient PSI-mediated electron transfer (Lohmann et al., 2006; Fatihi et al., 2015). Addition of vitamin K_1 in the medium allows to partially restore the growth of *Chlamydomonas men* mutants in high light, at the exception of *mena* (Figure 4). Although we cannot exclude the possibility that the inability of *Chlamydomonas mena* mutant to recover in the presence of vitamin K_1 is due to the partial deletion in the *HEL22* gene (coding for a DNA helicase RecQ), the fact that *Synechocystis mena* mutant is also unable to grow on medium supplemented with several naphthoquinone analogs (Johnson et al., 2001) rather suggests that MENA activity might be critical in the assimilation of exogenous phylloquinone. In this respect, it was demonstrated that *Mycobacterium tuberculosis* treated with a MenA inhibitor could not be rescued completely at high concentrations of exogenous vitamin K_2 (Kurosu and Begari, 2010). We thus hypothesize that the phytyl tail of exogenous PhQ is altered during its assimilation by the cells and that MENA is required to replace the altered phytyl chain. Although this activity has not been yet demonstrated in photosynthetic organisms, the human MenA homolog (UBIAD1) has both side-chain cleavage and prenylation activities (Nakagawa et al., 2010).

In *Chlamydomonas*, the main consequence of PhQ loss in *menc* (*phyllo*)*, mene, menb,* and *mena* mutants on the organization of the photosynthetic electron transfer chain is a decrease in the amount of functional PSI. This is consistent with the reduced PSI amount in *Synechocystis* mutants (Johnson et al., 2000; Sakuragi et al., 2002; Johnson et al., 2003). Replacement of PhQ by PQ leads to a reduced rate of electron transfer from A_1 to F_X (Lefebvre-Legendre et al., 2007; McConnell et al., 2011). In this respect, the specific increase in PSI antenna size in *men* mutants could represent a compensation mechanism linked to the decrease in the amount of active PSI centers. It was previously shown that polypeptides of PSI light harvesting complex (LHCA) accumulate at different levels and, it was suggested that flexibility in LHCA composition would allow adaptation of PSI antenna configuration to the prevailing environmental conditions (Stauber et al., 2009). PSII efficiency and maximum electron rate are however

diminished proportionally to PSI decrease in *Chlamydomonas men* mutants and these effects are exacerbated at higher light intensity where additional effect are observed like PSII . photoinhibition. Such PSIIphotoinhibition under high light has been also observed in *Arabidopsis meng* mutant (Lohmann et al., 2006). In high light, PSI activity in *men* mutants is obviously limited from acceptor side, a situation which has been described to lead to PSI photoinhibition and destruction in many studies (Munekage et al., 2002; Sommer et al., 2003; Tikkanen et al., 2015). Additionally, the redox state of the PQ pool is more reduced in high light and PQH_2 might occupy PS1 A_1 site in *men* mutant, as previously proposed in dark-anoxic conditions (McConnell et al., 2011). This might in turn further limit electron transfer and promote photoinhibition.

Critical role of phylloquinone in photosynthetic electron transfer in anoxia

The four *men* mutants isolated and described in this work were identified by an *in vivo* chlorophyll fluorescence imaging screen based on photosynthetic induction curves following transition from dark anoxia to light (Godaux et al., 2013). This *in vivo* chlorophyll fluorescence screen was originally used to detect mutants impaired in H_2 photoproduction (Godaux et al., 2013), a process that enables algae to initiate their photosynthetic electron transport chain after anoxic incubation when electron acceptor availability is scarce (Ghysels et al., 2013; Godaux et al., 2013; Clowez et al., 2015). The fluorescence transient observed for hydrogenase-deficient *hydg-2* mutant cells upon the first second of illumination in anoxia (Figure 6a) (Godaux et al., 2013) reflects the reduction phase of PSI acceptors (oxidized ferredoxin and $NADP^+$). Conversely, the lack of chlorophyll fluorescence changes for *men* mutant in anoxia probably indicates the absence of electron transfer between $P700^+$ and ferredoxin. This is in agreement with the proposal that PQH_2 replaces PhQ in the A_1 site of PSI in anoxia and prevents photosynthetic electron transfer in *mend* mutant (McConnell et al., 2011). As a result, long term reactivation (>5 min) of PSII electron transfer in anoxia, which relies on both PSI-dependant hydrogenase activity and PGRL1-dependant PSI cyclic electron flow in *Chlamydomonas* wild-type cells (Godaux et al., 2015), is fully compromised in *men* mutant (Figure 6b). PhQ loss thus severely impairs electron transfer in anoxia in our *men* mutants, as it was already shown in *mend* mutant (Lefebvre-Legendre et al., 2007;

McConnell et al., 2011). Overall these results indicate that the presence of PhQ as PSI A_1 cofactor is critical in photosynthetic organisms that encounter O_2-deprived conditions on a regular basis.

(6) EXPERIMENTAL PROCEDURES (1274 words)

Strains and growth conditions

The $4A^+$ (*mt*$^+$) and 2' (*mt*$^-$) wild-type strains used for transformation and genetic crosses, respectively, derive from 137c reference wild-type strain. The *mend* mutant (Lefebvre-Legendre et al., 2007) was provided by Kevin Redding (Arizona State University, United States). *C. reinhardtii* strains were grown in Tris-acetate-phosphate (TAP) medium (Harris et al., 1989) at 25°C under continuous white light (25 µmol photons m^{-2} s^{-1}), either on solid (1.5% agar) or liquid medium.

Insertional mutagenesis and fluorescence screening procedure

$4A^+$ cells were electroporated with 10 µg of DNA carrier and 250 ng of hygromycin B (*APHVII*) or paromomycin (*APHVIII*) resistance cassettes as previously described (Shimogawara et al., 1998). *APHVII* and *APHVIII* cassettes were amplified by PCR from pHyg3 (Berthold et al., 2002) or pSL18 (Depège et al., 2003) plasmids, respectively, as described in (Barbieri et al., 2011) using primers pairs APH7-F/APH7-R for *APHVII* and APH8-F/APH8-R for *APHVIII* (Table S2). Transformants were selected on TAP agar medium containing 25 µg/ml of hygromycin B or paromomycin in the light. After incubation of 5 to 10 days under light, transformants were screened directly on transformation plates according to a published procedure (Godaux et al., 2013) where anoxia is reached by incubation in anoxic bags (Anaerocult P, Merck).

DNA extraction, PCR amplifications, and TAIL-PCR

Total DNA was extracted using the procedure of (Newman et al., 1990). PCR amplifications were performed according standard protocols using Taq polymerase (Promega) or KAPA HIFI DNA polymerase (KAPA Biosystems, http://www.kapabiosystems.com) in case of amplification of *MENB* and *MENE* genes using primers menB-F3/menB-R1 and menE-F3/menE-R, respectively (Table S2). Amplification of insertion-linked sequence by thermal asymmetric interlaced (TAIL)-PCR was performed as described previously (Dent et al., 2005) using AD1, AD2 (Liu et al., 1995), RMD227 and RMD228 (Dent et al., 2005) as non-specific primers. For *APHVII*, the specific primers for primary, secondary and tertiary reactions were respectively APH7-R3, APH7-R4, and APH7-R5 at the 5' and HygTerm1, HygTerm2, and HygTerm3 at the 3' end of the coding sequence of the cassette (Table S2). For *APHVIII*, the specific primers for primary, secondary and tertiary reactions were respectively ParoTermB, ParoTermC/1, and ParoTerm2 at the 3' end of the coding sequence of the cassette (Table S2). PCR products were sequenced by Beckman Coulter Genomics and aligned to the *Chlamydomonas* genome sequence database (v5.5 on Phytozome v11.0).

Genetic analyses

Genetic crosses were performed as described in (Duby and Matagne, 1999). Zygotes were matured for 3 to 4 days under continuous light on nitrogen-free minimal agar plates. After maturation, blocks of agar carrying 50-100 zygotes were transferred to fresh TAP agar plates and exposed to chloroform vapours during 30 s. Germination was induced by exposure to light and nitrogen restoration. After 10 days of culture, 150-300 meiotic clones were randomly sampled and linkage analysis between resistance cassette and photosynthetic deficiency was determined using the protocol described previously (Godaux et al., 2013).

DNA gel blot analysis

Total DNA from wild-type and mutants cells were digested with *Stu*I and *Pst*I restriction enzymes (Thermo Scientific, Fast digest) which do not cut into *APHVII* or

APHVIII cassettes. DNA was separated on agarose gel, blotted to Hybond-N membranes (Amersham) and hybridized using digoxigenin-labeled probes (Duby and Matagne, 1999). Probes used to detect *APHVII* and *APHVIII* cassette were amplified by PCR with primers HygTail2 and APH7-R2 and pAPH-8F and pAPH-8R (Table S2) using Dig-11 dUTP, according to the procedure recommended by the manufacturer (Roche).

Spectroscopy

For all experiments, cells grown in low light (25 µmol photons m^{-2} s^{-1}), were harvested during exponential growth phase (3-5 x 10^6 cells/ml) and concentrated to a concentration of 10 µg chlorophyll/ml in fresh TAP medium.

In vivo chlorophyll fluorescence measurements were performed at room temperature using a fluorescence spectrophotometer (JTS-10, Biologic) or a fluorescence imaging setup (Speedzen-2, BEAMBIO). Actinic light was provided by light sources peaking at 640 nm and 520 nm, respectively. The effective photochemical yield of PSII (ΦPSII) was calculated as $(F_m' - F_s)/F_m'$, where F_s is the fluorescence level excited by actinic light (I_{lum}), and F_m' is the maximum fluorescence emission level induced by a 150-ms superimposed pulse of saturating light (> 3500 µmol photons m^{-2} s^{-1}). The relative electron transfer rate is obtained as $rETR_{II}$ = ΦPSII x I_{lum} (Genty et al., 1989).

Fluorescence emission spectra at 77K were recorded using a homebuilt spectrophotometer, based on a detecting diode array (AVS-USB 200; Ocean Optics). The excitation wavelength was provided by a LED source peaking at 440 nm. Cells were treated to induce state transitions before freezing in liquid nitrogen. PSII inhibitor DCMU (20 µM) was added for 20 min in the light used to promote state I.

The ratio between active PSI and PSII centers was estimated as previously described (Godaux et al., 2015) on cells adapted to dark for 30 min. Briefly, the amplitude of the fast phase (<1 ms) of the ECS signal (at 520–546 nm) after illumination with a single-turnover laser flash was monitored with a JTS-10 spectrophotometer (Biologic, France). The contribution of PSII was calculated from the decrease in the ECS amplitude after the flash upon the addition of the PSII inhibitors DCMU (20 µM) and hydroxylamine (1 mM), whereas the contribution of PSI corresponded to the amplitude of the ECS that

was insensitive to these inhibitors. PSI relative content was also assessed by measuring P_{700} absorption changes with a probing light peaking at 705 nm (6 nm full width at half maximum). In order to remove unspecific contributions to the signal at 705 nm, absorption changes measured at 740 nm (10 nm full width at half maximum) were subtracted. To fully reduce P_{700}, actinic light was provided by LED light sources (~1000 µmol photons m^{-2} s^{-1}) peaking at 640 nm in the presence of DCMU (20 µM) and hydroxylamine (1 mM).

Functional PSI antenna size was measured as the photon absorption rates of PSI (s^{-1} PS^{-1}) by recording the initial rate of ECS at the onset of actinic light in the presence of PSII inhibitors DCMU (20µM) and hydroxylamine (1mM) (Roberty et al., 2014). The slope was then normalized on ECS values corresponding to one charge separation per PSI.

Western blot analysis

The cell pellet corresponding to 1.5 ml of cell culture was suspended in extraction buffer (SDS 10%, glycerol 10%, 0.1 M DTT, 0.06 M Tris pH 6.8) to a final concentration of 1 µg protein/µl and incubated for 5 min at 100°C. Samples (5 µg) were then loaded in 10% SDS acrylamide gel and electroblotted according to standard protocols onto PVDF membranes (Amersham GE Healtcare, Buckinghamshire, England). Detection was performed using a Chemiluminescence Western blotting kit (Roche, Basel, Switzerland) with anti-rabbit peroxidase conjugated antibodies. Commercial rabbit antibodies (Agrisera) against PsaA (1:10,000), PsbC (1:30,000), and Cytochrome *f* (1:10,000) were used.

Pigment analyses

Pigments were extracted from whole cells in 90% (v/v) methanol, and debris were removed by centrifugation at 10,000 x g. Chlorophyll a + b concentration was determined with a λ 20 spectrophotometer (Perkin Elmer). Pigments and quinones were extracted from lyophilized cells with N,N-dimethylformamide (DMF) (Furuya et al., 1998). The resulting extracts were applied to an Acquity UPLC BEH C18 column (1.7 µm, 2.1 mm x 150 mm, Waters) at 40°C and were separated at a flow rate of 0.3 ml/min

using an UPLC (Acquity UPLC I-Class system, Waters) coupled with tandem mass spectrometry (Q Exactive, Thermo Scientific). The elution liquid gradient was generated as the following steps using solvent A (formic acid : water = 0.1 : 99.9) and solvent B (methanol): 0-5 min, 15%A/85%B to 5%A/95%B, hold to 9 min; 9-10 min, 5%A/95%B to 100%B, hold to 11.5 min; 11.5-12 min, 100%B to 15%A/85%B. The injection volume was 1 µl. Mass spectroscopy measurements were performed in a positive mode ESI.

(7) ACCESSION NUMBERS (7 words)

Accession numbers are listed in Table 1.

(8) ACKNOWLEDGMENTS (121 words)

We thank K. E. Redding for providing the *mend* strain of *C. reinhardtii*, the laboratory of K. K. Niyogi for providing $4A^{+}$ wild-type strain, G. Eppe & A. Marée for their technical help in UPLC-MS analyses, Y. Takahashi for advices on PhQ extraction method, E. Perez for her help in the identification of putative PTS, F. Franck for assay of PhQ analysis by HPLC, and M. Radoux for expert technical assistance. P.C acknowledges financial support from the Belgian Fonds de la Recherche Scientifique F.R.S.-F.N.R.S. (FRFC 2.4597, CDR J.0032, CDR J.0079 and Incentive Grant for Scientific Research F.4520) and from European Research Council (H2020-EU BEAL project 682580). B.E-A is supported by the Belgian FRIA F.R.S.-FNRS. P.C is a Research Associate from F.R.S.-FNRS.

(9) SHORT LEGENDS FOR SUPPORTING INFORMATION (141 words)

Figure S1: TAIL-PCR product sequences

Figure S2: Amplification of *MENB* and *MENE* genes and their flanking regions

Figure S3: Chlorophyll fluorescence induction curves of wild-type and complemented strains

Figure S4: PSI relative content

Figure S5: Determination of PSI and PSII antenna size in wild-type, complemented and *men* mutant strains

Figure S6: PSI and PSII content in control and mutant strains

Figure S7: RT-PCR analysis of *menc* and *mend* mutants

Figure S8: Sequence alignment of PHYLLO protein from *C. reinhardtii* (CrPHYLLO) and *A. thaliana* (AtPHYLLO) with *E. coli* MenF, MenD, MenC and MenH proteins (EcMenF, -D, -C, -H)

Figure S9: Sequence alignment of CYP25 protein from *C. reinhardtii* (CrCYP25) with its two homologs in humans (HsCYP4F2 and CYP4F11)

Table S1: Cosegregation analysis of the antibiotic resistance cassette with the fluorescence phenotype

Table S2: Primers sequences

Appendix S1: Detailed description of TAIL-PCR analyses

(10) REFERENCES (2077 words)

Babujee L, Wurtz V, Ma C, Lueder F, Soni P, Van Dorsselaer A, Reumann S (2010) The proteome map of spinach leaf peroxisomes indicates partial compartmentalization of phylloquinone (vitamin K1) biosynthesis in plant peroxisomes. J Exp Bot **61**: 1441–1453

Bailleul B, Cardol P, Breyton C, Finazzi G (2010) Electrochromism: a useful probe to study algal photosynthesis. Photosynth Res **106**: 179–189

Barbieri MR, Larosa V, Nouet C, Subrahmanian N, Remacle C, Hamel PP (2011) A Forward Genetic Screen Identifies Mutants Deficient for Mitochondrial Complex I Assembly in Chlamydomonas reinhardtii. Genetics **188**: 349–358

Berthold P, Schmitt R, Mages W (2002) An engineered Streptomyces hygroscopicus aph 7" gene mediates dominant resistance against hygromycin B in Chlamydomonas reinhardtii. Protist **153**: 401–412

Cardol P, Gloire G, Havaux M, Remacle C, Matagne R, Franck F (2003) Photosynthesis and state transitions in mitochondrial mutants of Chlamydomonas reinhardtii affected in respiration. Plant Physiol **133**: 2010–2020

Chen M, Ma X, Chen X, Jiang M, Song H, Guo Z (2013) Identification of a Hotdog Fold Thioesterase Involved in the Biosynthesis of Menaquinone in Escherichia coli. J Bacteriol **195**: 2768–2775

Clowez S, Godaux D, Cardol P, Wollman F-A, Rappaport F (2015) The involvement of hydrogen-producing and ATP-dependent NADPH-consuming

pathways in setting the redox poise in the chloroplast of Chlamydomonas reinhardtii in anoxia. J Biol Chem **290**: 8666–8676

Dent RM, Haglund CM, Chin BL, Kobayashi MC, Niyogi KK (2005) Functional genomics of eukaryotic photosynthesis using insertional mutagenesis of Chlamydomonas reinhardtii. Plant Physiol **137**: 545–556

Depège N, Bellafiore S, Rochaix J-D (2003) Role of chloroplast protein kinase Stt7 in LHCII phosphorylation and state transition in Chlamydomonas. Science **299**: 1572–1575

Desplats C, Mus F, Cuiné S, Billon E, Cournac L, Peltier G (2009) Characterization of Nda2, a plastoquinone-reducing type II NAD(P)H dehydrogenase in chlamydomonas chloroplasts. J Biol Chem **284**: 4148–4157

Drop B, Webber-Birungi M, Fusetti F, Kouřil R, Redding KE, Boekema EJ, Croce R (2011) Photosystem I of Chlamydomonas reinhardtii contains nine light-harvesting complexes (Lhca) located on one side of the core. J Biol Chem **286**: 44878–44887

Duby F, Matagne RF (1999) Alteration of dark respiration and reduction of phototrophic growth in a mitochondrial DNA deletion mutant of Chlamydomonas lacking cob, nd4, and the 3' end of nd5. Plant Cell **11**: 115–125

Edson KZ, Prasad B, Unadkat JD, Suhara Y, Okano T, Guengerich FP, Rettie AE (2013) Cytochrome P450-dependent catabolism of vitamin K: ω-hydroxylation catalyzed by human CYP4F2 and CYP4F11. Biochemistry **52**: 8276–8285

Fatihi A, Latimer S, Schmollinger S, Block A, Dussault PH, Vermaas WFJ (2015) A Dedicated Type II NADPH Dehydrogenase Performs the Penultimate Step in the Biosynthesis of Vitamin K 1 in Synechocystis and Arabidopsis. Plant Cell **27**: 1730–1741

Furt F, Allen WJ, Widhalm JR, Madzelan P, Rizzo RC, Basset G, Wilson MA (2013) Functional convergence of structurally distinct thioesterases from cyanobacteria and plants involved in phylloquinone biosynthesis. Acta Crystallogr Sect D Biol Crystallogr **69**: 1876–1888

Furuya K, Hayashi M, Yabushita Y (1998) HPLC Determination of Phytoplankton Pigments Using N,N-Dimethylformamide. J Oceanogr **54**: 199–203

Garcion C, Lohmann A, Lamodie E, Catinot J, Buchala A, Doermann P, Métraux J-P (2008) Characterization and Biological Function of the ISOCHORISMATE SYNTHASE2 Gene of Arabidopsis. Plant Physiol **147**: 1279–1287

Genty B, Briantais J-M, Baker NR (1989) The relationship between the quantum yield of photosynthetic electron transport and quenching of chlorophyll fluorescence. Biochim Biophys Acta **990**: 87–92

Ghysels B, Godaux D, Matagne RF, Cardol P, Franck F (2013) Function of the chloroplast hydrogenase in the microalga Chlamydomonas: the role of hydrogenase and state transitions during photosynthetic activation in anaerobiosis. PLoS One **8**: e64161

Godaux D, Bailleul B, Berne N, Cardol P (2015) Induction of photosynthetic carbon fixation in anoxia relies on hydrogenase activity and PGRL1-mediated cyclic electron flow in Chlamydomonas reinhardtii. Plant Physiol **168**: 648–658

Godaux D, Emonds-Alt B, Berne N, Ghysels B, Alric J, Remacle C, Cardol P (2013) A novel screening method for hydrogenase-deficient mutants in Chlamydomonas reinhardtii based on in vivo chlorophyll fluorescence and photosystem II quantum yield. Int J Hydrogen Energy **38**: 1826–1836

Gross J, Won KC, Lezhneva L, Falk J, Krupinska K, Shinozaki K, Seki M, Herrmann RG, Meurer J (2006) A plant locus essential for phylloquinone (vitamin K1) biosynthesis originated from a fusion of four eubacterial genes. J Biol Chem **281**: 17189–17196

Guergova-Kuras M, Boudreaux B, Joliot A, Joliot P, Redding K (2001) Evidence for two active branches for electron transfer in photosystem I. Proc Natl Acad Sci U S A **98**: 4437–4442

Harris EH, Burkhart BD, Gillham NW, Boynton JE (1989) Antibiotic resistance mutations in the chloroplast 16S and 23S rRNA genes of Chlamydomonas reinhardtii: correlation of genetic and physical maps of the chloroplast genome. Genetics **123**: 281–292

Hippler M, Redding K, Rochaix JD (1998) Chlamydomonas genetics, a tool for the study of bioenergetic pathways. Biochim Biophys Acta **1367**: 1–62

Ikeda Y, Komura M, Watanabe M, Minami C, Koike H, Itoh S, Kashino Y, Satoh K (2008) Photosystem I complexes associated with fucoxanthin-chlorophyll-binding proteins from a marine centric diatom, Chaetoceros gracilis. Biochim Biophys Acta - Bioenerg **1777**: 351–361

Jiang M, Cao Y, Guo Z, Chen M, Chen X, Guo Z (2007) Menaquinone Biosynthesis in Escherichia coli : Identification of 2-Succinyl-5-enolpyruvyl-6-hydroxy-3-cyclohexene-1-carboxylate as a Novel Intermediate and Re-Evaluation of MenD Activity †. Biochemistry **46**: 10979–10989

Jiang M, Chen X, Guo Z, Cao Y, Chen M, Guo Z (2008) Identification and Characterization of (1R, 6R) -2-Succinyl-6-hydroxy-2,4-cyclohexadiene-1-carboxylate Synthase in the Menaquinone Biosynthesis of Escherichia coli. Biochemistry **47**: 3426–3434

Johnson TW, Naithani S, Stewart C, Zybailov B, Jones a. D, Golbeck JH, Chitnis PR (2003) The menD and menE homologs code for 2-succinyl-6-hydroxyl-2,4-cyclohexadiene-1-carboxylate synthase and O-succinylbenzoic acid-CoA synthase in the phylloquinone biosynthetic pathway of Synechocystis sp. PCC 6803. Biochim Biophys Acta - Bioenerg **1557**: 67–76

Johnson TW, Shen G, Zybailov B, Kolling D, Reategui R, Beauparlant S, Vassiliev IR, Bryant DA, Jones D, Golbeck JH, et al (2000) Recruitment of a Foreign Quinone into the A1 Site of Photosystem I. I. GENETIC AND PHYSIOLOGICAL CHARACTERIZATION OF PHYLLOQUINONE BIOSYNTHETIC PATHWAY MUTANTS IN SYNECHOCYSTIS SP. PCC 6803. J Biol Chem **275**: 8523–8530

Johnson TW, Zybailov B, Jones a. D, Bittl R, Zech S, Stehlik D, Golbeck JH, Chitnis PR (2001) Recruitment of a foreign quinone into the A1 site of photosystem I: In vivo replacement of plastoquinone-9 by media-supplemented naphthoquinones in phylloquinone biosynthetic pathway mutants of synechocystis sp. PCC 6803. J Biol Chem **276**: 39512–39521

Joliot P, Joliot A (1999) In vivo analysis of the electron transfer within photosystem I: are the two phylloquinones involved? Biochemistry **38**: 11130–11136

Kim HU (2008) The AAE14 gene encodes the Arabidopsis o-succinylbenzoyl- CoA ligase that is essential for phylloquinone synthesis and photosystem-I function. Plant J **54**: 272–283

Kurosu M, Begari E (2010) Vitamin K2 in electron transport system: Are enzymes involved in vitamin K2 biosynthesis promising drug targets? Molecules **15**: 1531–1553

Lauersen KJ, Willamme R, Coosemans N, Joris M, Kruse O, Remacle C (2016) Peroxisomal microbodies are at the crossroads of acetate assimilation in the green microalga Chlamydomonas reinhardtii. Algal Res **16**: 266–274

Law A, Thomas G, Threlfall DR (1973) 5′-Monohydroxyphylloquinone from Anacystis and Euglena. Phytochemistry **12**: 1999–2004

Lefebvre-Legendre L, Rappaport F, Finazzi G, Ceol M, Grivet C, Hopfgartner G, Rochaix JD (2007) Loss of phylloquinone in Chlamydomonas affects plastoquinone pool size and photosystem II synthesis. J Biol Chem **282**: 13250–13263

Liu YG, Mitsukawa N, Oosumi T, Whittier RF (1995) Efficient isolation and mapping of Arabidopsis thaliana T-DNA insert junctions by thermal asymmetric interlaced PCR. Plant J **8**: 457–463

Lohmann A, Schöttler MA, Bréhélin C, Kessler F, Bock R, Cahoon EB, Dörmann P (2006) Deficiency in phylloquinone (vitamin K1) methylation affects prenyl quinone distribution, photosystem I abundance, and anthocyanin accumulation in the Arabidopsis AtmenG mutant. J Biol Chem **281**: 40461–40472

McConnell MD, Cowgill JB, Baker PL, Rappaport F, Redding KE (2011) Double reduction of plastoquinone to plastoquinol in Photosystem 1. Biochemistry **50**: 11034–11046

Meganathan R (2001) Biosynthesis of menaquinone (vitamin K2) and ubiquinone (coenzyme Q): a perspective on enzymatic mechanisms. Vitam Horm **61**: 173–218

Munekage Y, Hojo M, Meurer J, Endo T, Tasaka M, Shikanai T (2002) PGR5 is involved in cyclic electron flow around photosystem I and is essential for photoprotection in Arabidopsis. Cell **110**: 361–371

Nakagawa K, Hirota Y, Sawada N, Yuge N, Watanabe M, Uchino Y, Okuda N, Shimomura Y, Suhara Y, Okano T (2010) Identification of UBIAD1 as a novel human menaquinone-4 biosynthetic enzyme. Nature **468**: 117–121

Newman SM, Boynton JE, Gillham NW, Randolph-Anderson BL, Johnson a. M, Harris EH (1990) Transformation of chloroplast ribosomal RNA genes in Chlamydomonas: Molecular and genetic characterization of integration events. Genetics **126**: 875–888

Omata T, Murata N (1984) Cytochromes and prenylquinones in preparations of cytoplasmic and thylakoid membranes from the cyanobacterium (blue-green alga) Anacystis nidulans. Biochim Biophys Acta (BBA)-Bioenergetics **766**: 395–402

Ozawa SI, Kosugi M, Kashino Y, Sugimura T, Takahashi Y (2012) 5'-monohydroxyphylloquinone is the dominant naphthoquinone of PSI in the green alga chlamydomonas reinhardtii. Plant Cell Physiol **53**: 237–243

Reumann S, Babujee L, Ma C, Wienkoop S, Siemsen T, Antonicelli GE, Rasche N, Lüder F, Weckwerth W, Jahn O (2007) Proteome analysis of Arabidopsis leaf peroxisomes reveals novel targeting peptides, metabolic pathways, and defense mechanisms. Plant Cell **19**: 3170–3193

Roberty S, Bailleul B, Berne N, Franck F, Cardol P (2014) PSI Mehler reaction is the main alternative photosynthetic electron pathway in Symbiodinium sp., symbiotic dinoflagellates of cnidarians. New Phytol **204**: 81–91

Rochaix J-D (2002) Chlamydomonas, a model system for studying the assembly and dynamics of photosynthetic complexes. FEBS Lett **529**: 34–38

Sakuragi Y, Zybailov B, Shen G, Jones a D, Chitnis PR, Est A Van Der, Bittl R, Zech S, Stehlik D, Golbeck JH, et al (2002) Insertional Inactivation of the menG

Gene , Encoding 2-Phytyl-1 , 4-Naphthoquinone Methyltransferase of Synechocystis sp . PCC 6803 , Results in the Incorporation of 2-Phytyl-1 , 4-Naphthoquinone into the A 1 Site and Alteration of the Equilibrium Constan. Biochemistry **41**: 394–405

Semenov AY, Vassiliev IR, Van Der Est A, Mamedov MD, Zybailov B, Shen G, Stehlik D, Diner B a., Chitnis PR, Golbeck JH (2000) Recruitment of a foreign qiunone into the a(1) site of photosystem I: Altered kinetics of electron transfer in phylloquinone biosynthetic pathway mutants studied by time-resolved optical, EPR, and electrometric techniques. J Biol Chem **275**: 23429–23438

Shimada H, Ohno R, Shibata M, Ikegami I, Onai K, Ohto MA, Takamiya KI (2005) Inactivation and deficiency of core proteins of photosystems I and II caused by genetical phylloquinone and plastoquinone deficiency but retained lamellar structure in a T-DNA mutant of Arabidopsis. Plant J **41**: 627–637

Shimogawara K, Fujiwara S, Grossman A, Usuda H (1998) High-efficiency transformation of Chlamydomonas reinhardtii by electroporation. Genetics **148**: 1821–1828

Sommer F, Hippler M, Biehler K, Fischer N, Rochaix J-D (2003) Comparative analysis of photosensitivity in photosystem I donor and acceptor side mutants of Chlamydomonas reinhardtii. Plant, Cell Environ **26**: 1881–1892

Stauber EJ, Busch A, Naumann B, Svatos A, Hippler M (2009) Proteotypic profiling of LHCI from Chlamydomonas reinhardtii provides new insights into structure and function of the complex. Proteomics **9**: 398–408

Takahashi H, Clowez S, Wollman F-A, Vallon O, Rappaport F (2013) Cyclic electron flow is redox-controlled but independent of state transition. Nat Commun. **4**:1954 doi: 10.1038/ncomms2954

Tikkanen M, Rantala S, Aro E-M (2015) Electron flow from PSII to PSI under high light is controlled by PGR5 but not by PSBS. Front Plant Sci. doi: 10.3389/fpls.2015.00521

Widhalm JR, Ducluzeau AL, Buller NE, Elowsky CG, Olsen LJ, Basset GJC (2012) Phylloquinone (vitamin K1) biosynthesis in plants: Two peroxisomal thioesterases of lactobacillales origin hydrolyze 1,4-dihydroxy-2-naphthoyl-coa. Plant J **71**: 205–215

Widhalm JR, van Oostende C, Furt F, Basset GJC (2009) A dedicated thioesterase of the Hotdog-fold family is required for the biosynthesis of the naphthoquinone ring of vitamin K 1. Proc Natl Acad Sci U S A **106**: 5599–5603

Wollman FA (2001) State transitions reveal the dynamics and flexibility of the photosynthetic apparatus. EMBO J **20**: 3623–3630

Yoshida E, Nakamura A, Watanabe T (2003) Reversed-phase HPLC determination of chlorophyll a' and naphthoquinones in photosystem I of red algae: existence of two menaquinone-4 molecules in photosystem I of Cyanidium caldarium. Anal Sci **19**: 1001–5

Ziegler K, Maldener I, Lockau W (1989) 5′-Monohydroxyphylloquinone as a Component of Photosystem I. Zeitschrift fur Naturforsch - Sect C J Biosci **44**: 468–472

(11) TABLES (22 words)

Table 1: Menaquinone biosynthesis enzymes in *E. coli* and their homologs involved in the biosynthesis of PhQ in *Synechocystis*, *Arabidopsis* and *Chlamydomonas*.

	E.coli	*Synechocystis sp.* PCC6803	*A. thaliana*	*C. reinhardtii*	E-value[a]
Isochorismate synthase	MenF	Slr0817	At1g74710 (ICS1) At1g18870 (ICS2)	Cre16.g659050 (PHYLLO)	6.4E-74
SEPHCHC synthase	MenD	Sll0603	At1g68890 (PHYLLO)	Cre16.g659050 (PHYLLO)	6.4E-74
SHCHC synthase	MenH	Slr1916	At1g68890 (PHYLLO)	Cre16.g659050 (PHYLLO)	6.4E-74
OSB synthase	MenC	Sll0409	At1g68890 (PHYLLO)	Cre16.g659050 (PHYLLO)	6.4E-74
OSB-CoA ligase	MenE	Slr0492	At1g30520 (AAE14)	Cre01.g030900 (MENE)	1.3E-58
DHNA synthase	MenB	Sll1127	At1g60550 (NS)	Cre02.g114250 (MENB)	1.9E-151
DHNA-CoA thioesterase	YdiI	Slr0204	At1g48320 (AtDHNAT1) At5g48950 (AtDHNAT2)	Cre07.g323150[b] (TEH4) (putative)	-[b]
DHNA phytyltransferase	MenA	Slr1518	At1g60600 (ABC4)	Cre04.g219787 (MENA)	2.6E-14
Demethylphylloquinone oxidoreductase	-[c]	Slr1743 (NdbB)	At5g08740 (NDC1)	Cre16.g671000 (NDA5) (putative)	4.5E-73

Demethylphylloquinone methyltransferase	MenG	Sll1653	At1g23360 (AtMenG)	Cre02.g084300 (MENG) (putative)	3.3E-75

[a]E-values from BLAST analysis with *Arabidopis* protein sequences against *Chlamydomonas* genome (version 5.5).

[b]No homolog has been found in *C. reinhardtii* genomic database for the DHNA-CoA thioesterase described in *Synechocystis* and *Arabidopsis*. TEH4 is a putative candidate (see discussion for further details).

[c]The penultimate reduction step of PhQ biosynthesis has not yet been demonstrated in menaquinone biosynthesis in bacteria.

(12) FIGURES LEGENDS (809 words)

Figure 1: Chlorophyll fluorescence induction curves of wild-type and mutant strains.
Chlorophyll fluorescence induction curves upon illumination at ~ 110 µmol photons (λ = 520 nm) m^{-2} s^{-1} of *C. reinhardtii* wild type, *mend* mutant, and mutant strains identified in this work after acclimation to dark anoxic (>12 h) (a-b) and oxic conditions (c). Arrows indicate when the saturating light pulse was given.

Figure 2: Molecular characterization of the mutants.
(a) DNA-blot analysis of wild-type and mutant strains. For AO1, AS1 and AS2, DNA-blot was hybridized with dig-labelled *APHVII* probe while for 25.1 DNA-blot was hybridized with *APHVIII* dig-labelled probe. (b) Organization and structure of the *MENA*, *MENB*, *MENE*, and *PHYLLO* genes as shown in *C. reinhardtii* genome version 5.5 available at http://phytozome.org (black boxes, exons; black lines, introns; grey boxes, 5' and 3' UTRs; *men*-homologous regions, black pointer), and localization of the antibiotic resistance cassette (diagonally hatched arrows, *APHVII*; vertically hatched arrows, *APHVII*; white arrows, pieces of non-functional cassette).

Figure 3: Analysis of phylloquinone content by UPLC-MS.

Detection of 5'-monohydroxyphylloquinone (selected monitoring mode, m/z= 488.5-489.5, retention time: ~8 min) from wild type, complemented strains (*menbR*, *meneR*) and *men* mutants. Values are normalized to the relative abundance of lutein (m/z=568.43).

Figure 4: Growth of control and mutant strains under different culture conditions.
Growth patterns of wild type, complemented strains and *men* mutants. 20 µl of cell culture at 10^6 cells/ml were plated on acetate-containing medium (TAP), acetate-free medium (TMP) and TAP medium supplemented with 5 µM of phylloquinone (PhQ). Agar plates were incubated for 3 and 7 days under 0, 25, 75, 125 and 300 µmol photons m^{-2} s^{-1}. The images for each experimental condition come from a single petri dish with all strains, except *menc* which was compared to wild type only.

Figure 5: Photosystem content, antenna size, and electron transfer rate in control and mutant strains.
(a,b) Active PSI and PSII content was estimated from electrochromic shift signals (ECS) at 520-546 nm on cells grown in low light (a) and then transferred for four hours at high light intensity (HL, 400 µmol photons m^{-2} s^{-1}) (b). Active PSI centers content of wild-type cells was normalized to 1. Values are the average of three independent experiments. (c, d) Immunoblots against *C. reinhardtii* PsaA,Cp43, and cytochrome *f* proteins of total cell extracts (5 µg per lane) prepared from wild-type, *menbR*, *meneR*, *mena*, *menb*, *menc*, *mend* and *mene* cells grown in low light (c) and then transferred for four hours at high light (400 µmol photons m^{-2} s^{-1}) (d). The antibodies used are indicated. (e, f) PSII relative electron transfer rate ($rETR_{II}$, µmol e^- s^{-1} m^{-2}) as a function of the light intensity (I, µmol photons m^{-2} s^{-1}) of cells grown in low light (e) and then transferred for four hours at high light (400 µmol photons m^{-2} s^{-1}) (f). (e, f) Values are the average of ten independent experiments. (g) F715 to F685 ratio from fluorescence emissions spectra at 77 K. Different pretreatments were applied to cell suspensions before freezing: control under white light of 25 µmol photons m^{-2} s^{-1} ("no add", dark grey symbols) or illumination by white light of 25 µmol photons m^{-2} s^{-1} in the presence of 20 µM DCMU ("light + DCMU", light grey symbols). (h) PSI antenna size estimated from ECS absorbance transients (520-546 nm) in DCMU (20 µM) + hydroxylamine (1

mM) - poisoned cells (Figure S5a). PSII antenna size estimated from chlorophyll fluorescence transients in DCMU (20 µM) - poisoned cells (Figure S5b). (g-h) Wild-type values were normalized to 1 and all values are the average of three independent experiments.

Figure 6: Reactivation of photosynthesis after dark anoxia acclimation.
(a) Chlorophyll fluorescence induction curves upon illumination at ~ 110 µmol photons (λ = 520 nm) m^{-2} s^{-1} of *C. reinhardtii* wild-type, hydrogenase-deficient (*hydg-2*), *menb* mutant and *menbR* complemented strains after acclimation to dark anoxic (220 min). (b) Evolution of PSII quantum yield (ΦPSII) following a shift from dark anoxia to light (250 µmol photons m^{-2} s^{-1}) of *C. reinhardtii* wild-type, hydrogenase-deficient (*hydg-2*), *menb* mutant and *menbR* complemented strains.

Figure 7: Phylloquinone biosynthetic pathway in *Chlamydomonas reinhardtii*.
The gene products encoding each step in *Chlamydomonas* are indicated. The PHYLLO protein contains catalytic domains corresponding to MenF, MenD, MenH and MenC of the menaquinone pathway. MENE, MENB, and TEH4 possess peroxisome targeting sequences suggesting a compartmentalized phylloquinone biosynthesis pathway similar to that of land plants (see text for details). Solid black boxes indicate that mutants have been characterized, dotted black boxes specify putative *men* proteins and grey arrows designate uncharacterized membrane trafficking steps (see text for details). MenF, isochorismate synthase; MenD, SEPHCHC synthase; MenH, SHCHC synthase; MenC, OSB synthase; MenE, OSB-CoA ligase; MenB, DHNA synthase; MenA, DHNA phytyltransferase; TEH4, DHNAT, putative DHNA-CoA thioesterase; Nda5, demethylphylloquinone oxidoreductase; MenG, demethylphylloquinone methyltransferase. SEPHCHC, 2-succinyl-5-enolpyruvyl-6-hydroxy-3-cyclohexene-1-carboxylic acid; SHCHC, 2-succinyl-6-hydroxy-2,4-cyclohexadiene-1-carboxylic acid.; OSB, o-succinylbenzoic acid; DHNA, 1,4-dihydroxy-2-naphtoate, CYP25, putative phylloquinone hydroxylase.

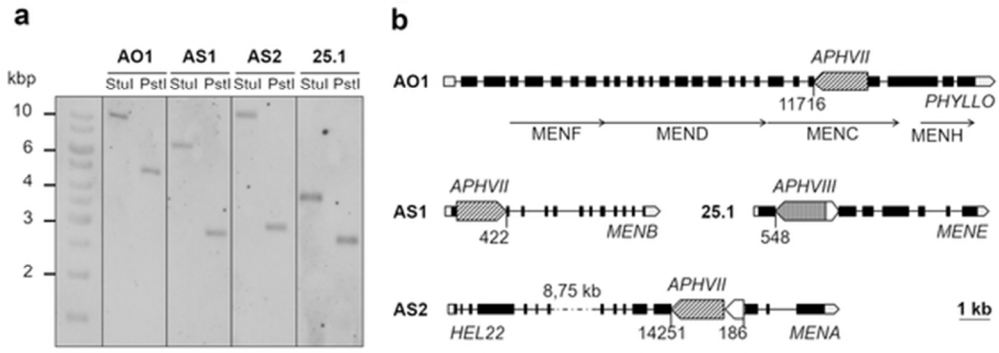

Figure 2: Molecular characterization of the mutants.
(a) DNA-blot analysis of wild-type and mutant strains. For AO1, AS1 and AS2, DNA-blot was hybridized with dig-labelled APHVII probe while for 25.1 DNA-blot was hybridized with APHVIII dig-labelled probe. (b) Organization and structure of the MENA, MENB, MENE, and PHYLLO genes as shown in *C. reinhardtii* genome version 5.5 available at http://phytozome.org (black boxes, exons; black lines, introns; grey boxes, 5' and 3' UTRs; men-homologous regions, black pointer), and localization of the antibiotic resistance cassette (diagonally hatched arrows, APHVII; vertically hatched arrows, APHVII; white arrows, pieces of non-functional cassette).

Figure 2
51x18mm (300 x 300 DPI)

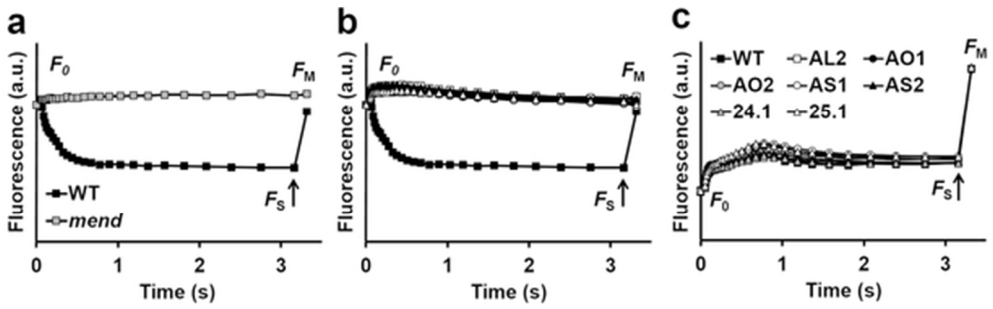

Figure 1: Chlorophyll fluorescence induction curves of wild-type and mutant strains.‼ ┼ Chlorophyll fluorescence induction curves upon illumination at ~ 110 µmol photons (λ = 520 nm) m^{-2} s^{-1} of *C. reinhardtii* wild type, *mend* mutant, and mutant strains identified in this work after acclimation to dark anoxic (>12 h) (a-b) and oxic conditions (c). Arrows indicate when the saturating light pulse was given. ‼ ┼
Figure 1
52x16mm (300 x 300 DPI)

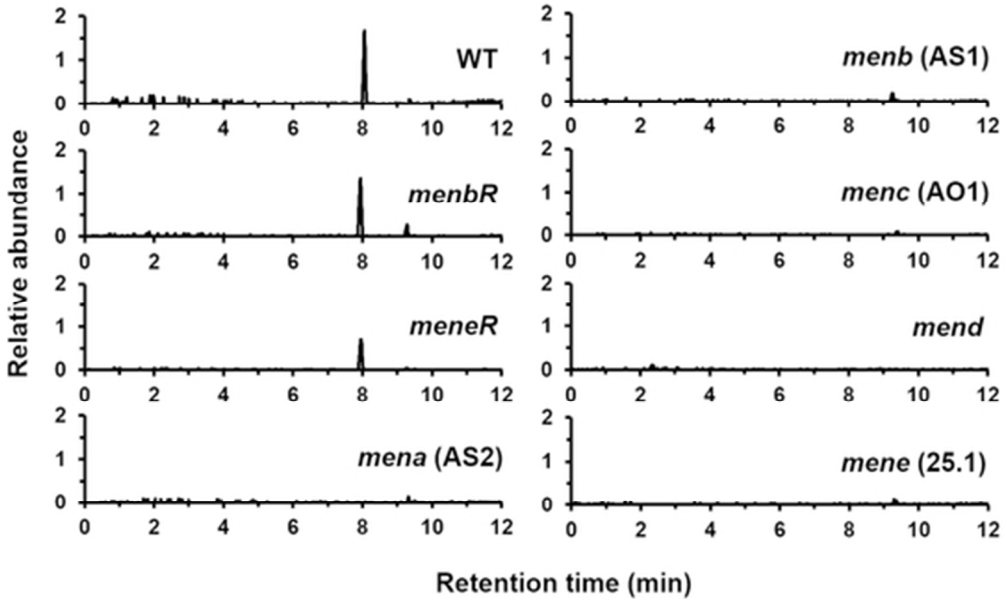

Figure 3: Analysis of phylloquinone content by UPLC-MS.‼ ┼ Detection of 5'-monohydroxyphylloquinone (selected monitoring mode, m/z= 488.5-489.5, retention time: ~8 min) from wild type, complemented strains (*menbR, meneR*) and *men* mutants. Values are normalized to the relative abundance of lutein (m/z=568.43).‼ ┼

Figure 3
45x27mm (300 x 300 DPI)

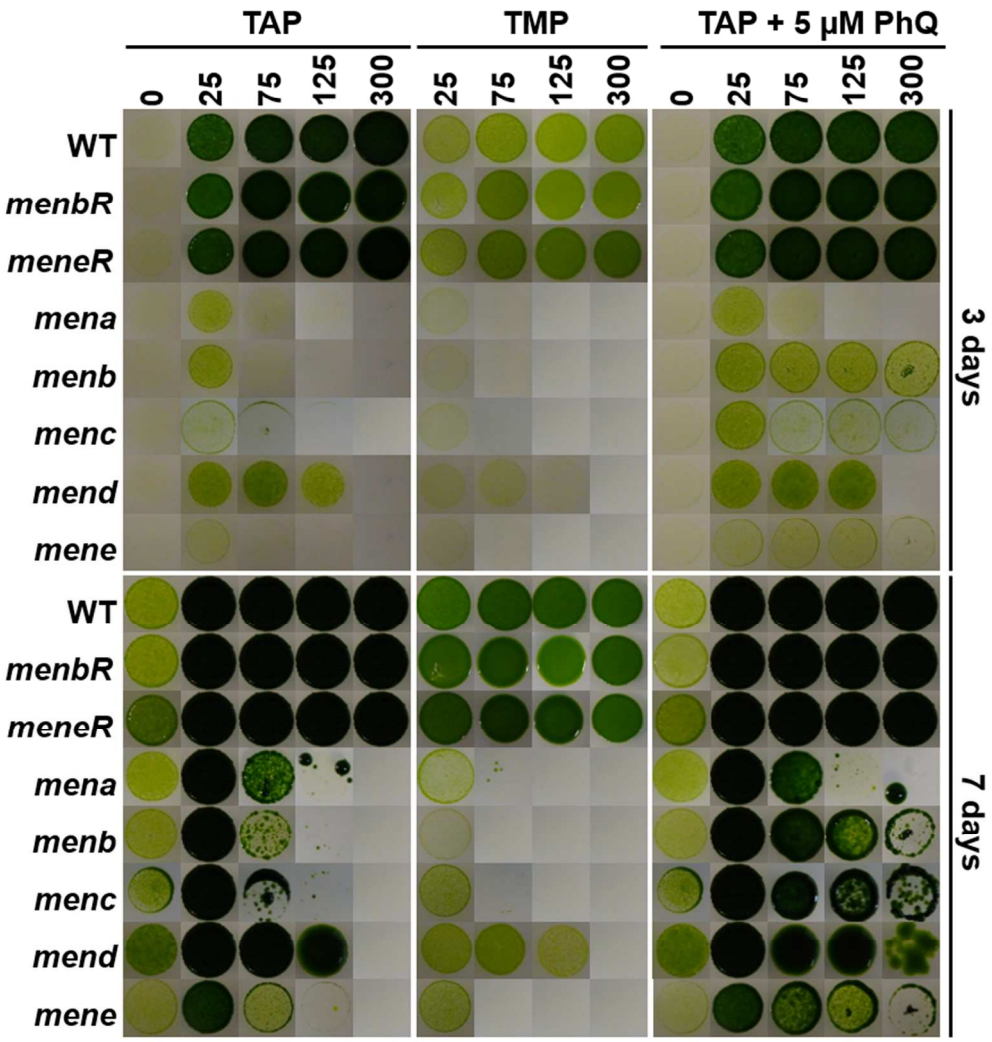

Figure 4: Growth of control and mutant strains under different culture conditions.‼ ┼ Growth patterns of wild type, complemented strains and *men* mutants. 20 µl of cell culture at 106 cells/ml were plated on acetate-containing medium (TAP), acetate-free medium (TMP) and TAP medium supplemented with 5 µM of phylloquinone (PhQ). Agar plates were incubated for 3 and 7 days under 0, 25, 75, 125 and 300 µmol photons m^{-2} s^{-1}. The images for each experimental condition come from a single petri dish with all strains, except *menc* which was compared to wild type only.‼ ┼

Figure 4
74x78mm (300 x 300 DPI)

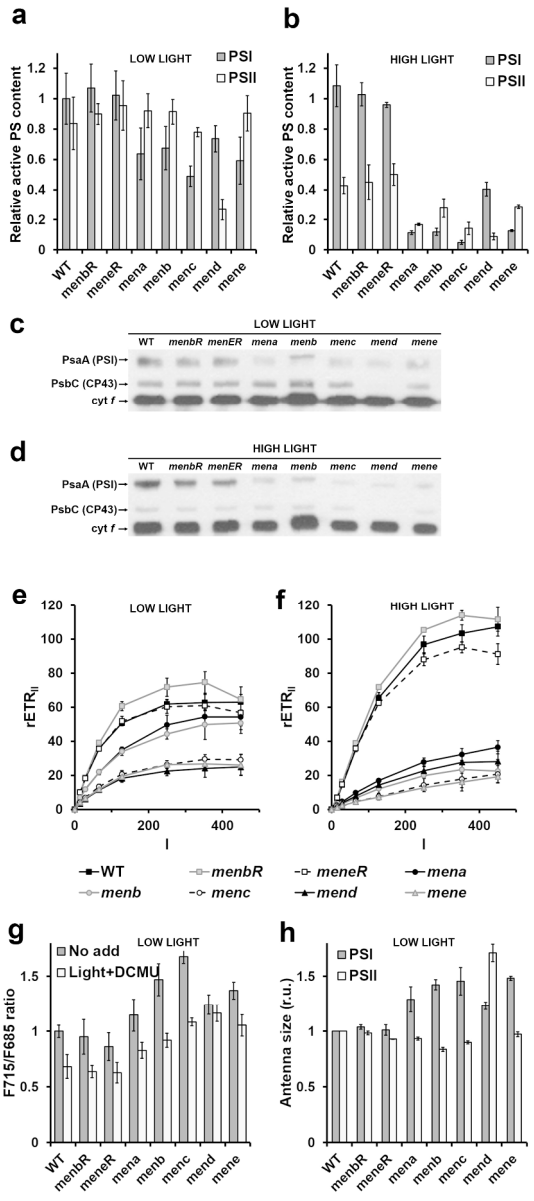

Figure 5: Photosystem content, antenna size, and electron transfer rate in control and mutant strains. %"(a,b) Active PSI and PSII content was estimated from electrochromic shift signals (ECS) at 520-546 nm on cells grown in low light (a) and then transferred for four hours at high light intensity (HL, 400 µmol photons m^{-2} s^{-1}) (b). Active PSI centers content of wild-type cells was normalized to 1. Values are the average of three independent experiments. (c, d) Immunoblots against C. reinhardtii PsaA,Cp43, and cytochrome f proteins of total cell extracts (5 µg per lane) prepared from wild-type, *menbR*, *meneR, mena, menb, menc, mend* and *mene* cells grown in low light (c) and then transferred for four hours at high light (400 µmol photons m^{-2} s^{-1}) (d). The antibodies used are indicated. (e, f) PSII relative electron transfer rate (rETRII, µmol e^{-} s^{-1} m^{-2}) as a function of the light intensity (I, µmol photons m^{-2} s^{-1}) of cells grown in low light (e) and then transferred for four hours at high light (400 µmol photons m^{-2} s^{-1}) (f). (e, f) Values are the average of ten independent experiments. (g) F715 to F685 ratio from fluorescence emissions spectra at 77 K. Different pretreatments were applied to cell suspensions before freezing: control under white light of 25 µmol photons m^{-2} s^{-1} ("no add", dark grey symbols) or illumination by white light of 25 µmol photons m^{-2} s^{-1}

in the presence of 20 µM DCMU ("light + DCMU", light grey symbols). (h) PSI antenna size estimated from ECS absorbance transients (520-546 nm) in DCMU (20 µM) + hydroxylamine (1 mM) - poisoned cells (Figure S5a). PSII antenna size estimated from chlorophyll fluorescence transients in DCMU (20 µM) - poisoned cells (Figure S5b). (g-h) Wild-type values were normalized to 1 and all values are the average of three independent experiments. %"

Figure 5

179x406mm (300 x 300 DPI)

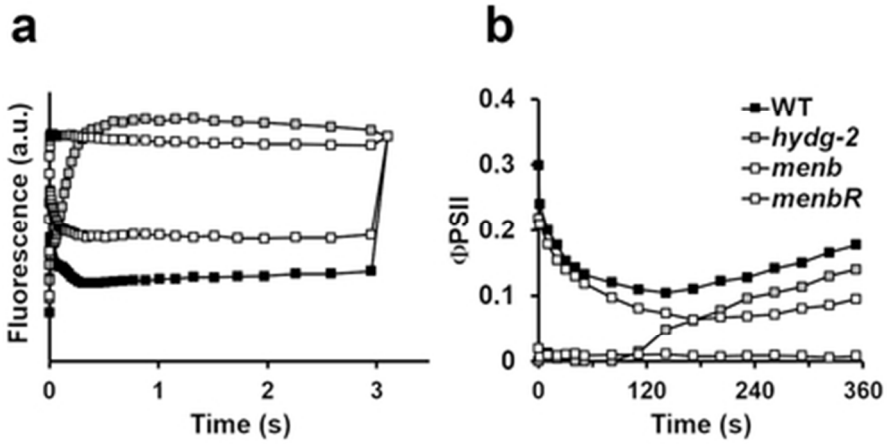

Figure 6: Reactivation of photosynthesis after dark anoxia acclimation.
(a) Chlorophyll fluorescence induction curves upon illumination at ~ 110 µmol photons (λ = 520 nm) m^{-2} s^{-1} of *C. reinhardtii* wild-type, hydrogenase-deficient (*hydg-2), menb* mutant and *menbR* complemented strains after acclimation to dark anoxic (220 min). (b) Evolution of PSII quantum yield (ΦPSII) following a shift from dark anoxia to light (250 µmol photons m^{-2} s^{-1}) of *C. reinhardtii* wild-type, hydrogenase-deficient (*hydg-2*), *menb* mutant and *menbR* complemented strains.

Figure 6
37x18mm (300 x 300 DPI)

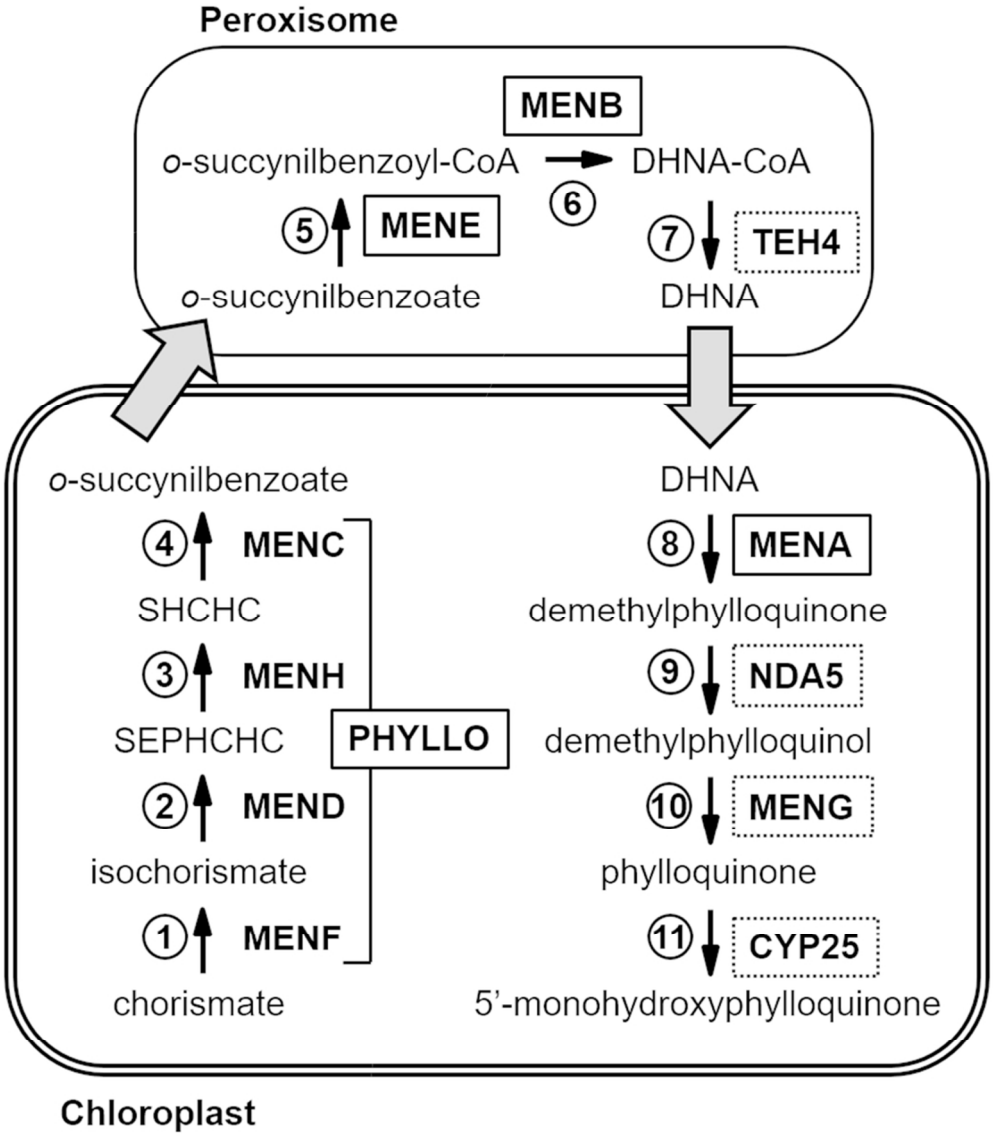

Figure 7: Phylloquinone biosynthetic pathway in *Chlamydomonas reinhardtii.*
The gene products encoding each step in Chlamydomonas are indicated. The PHYLLO protein contains catalytic domains corresponding to MenF, MenD, MenH and MenC of the menaquinone pathway. MENE, MENB, and TEH4 possess peroxisome targeting sequences suggesting a compartmentalized phylloquinone biosynthesis pathway similar to that of land plants (see text for details). Solid black boxes indicate that mutants have been characterized, dotted black boxes specify putative men proteins and grey arrows designate uncharacterized membrane trafficking steps (see text for details). MenF, isochorismate synthase; MenD, SEPHCHC synthase; MenH, SHCHC synthase; MenC, OSB synthase; MenE, OSB-CoA ligase; MenB, DHNA synthase; MenA, DHNA phytyltransferase; TEH4, DHNAT, putative DHNA-CoA thioesterase; Nda5, demethylphylloquinone oxidoreductase; MenG, demethylphylloquinone methyltransferase. SEPHCHC, 2-succinyl-5-enolpyruvyl-6-hydroxy-3-cyclohexene-1-carboxylic acid; SHCHC, 2-succinyl-6-hydroxy-2,4-cyclohexadiene-1-carboxylic acid.; OSB, o-succinylbenzoic acid; DHNA, 1,4-dihydroxy-2-naphtoate, CYP25, putative phylloquinone hydroxylase.

Figure 7

89x104mm (300 x 300 DPI)

Appendix S1: Detailed description of TAIL-PCR analysis.

TAIL-PCR products were obtained at the 3' end of the resistance cassette for AO1, AS1 and 25.1 mutants and at both ends for AS2 mutant. In AO1 mutant, the PCR sequence contains 273 bp of the 3' end of *APHVII* and 459 bp of *PHYLLO* gene (Cre16.g659050, 15,756 bp) (Figure S1), allowing us to localize the 3' end of the cassette at position 11,716 of *PHYLLO* gene in MENC catalytic domain (Figure 2b). In AS1 mutant, the TAIL-PCR product contains 101 bp of the 3' end of the *APHVII* cassette and 693 bp of the *MENB* gene (Cre02.g114250, 5,066 bp) (Figure S1), allowing us to localize the 3' end of the cassette at position 422 of *MENB* gene (Figure 2b). In AS2 mutant, the sequence of the TAIL-PCR products (Figure S1) allowed us to localize the 5' end of *APHVII* at position 186 in *MENA* gene (Cre04.g219787, 3,136 bp) and the 3' of *APHVII* at position 14,251 in the neighbouring gene coding for *HEL22* DNA helicase RecQ (Cre04.g219750, 14,531 bp). The cassette insertion caused a deletion of 514 bp in AS2 genome (279 bp of *HEL22*, 49 bp of intergenic sequence and 186 bp of *MENA*). Additional PCR analysis showed a piece of non-functional cassette (597 bp) upstream of the 5' end of *APHVII* functional cassette in AS2 (Figure 2b). Finally, in 25.1 mutant, the PCR sequence contains 259 bp of the 3' end of *APHVIII* and 535 bp of *MENE* (Cre01.g030900, 3,986 bp) (Figure S1), allowing us to localize the 3' end of the cassette at position 548 of *MENE* gene. Additional PCR analysis showed a piece of non-functional cassette (477 bp) upstream of the 5' end of *APHVIII* functional cassette in 25.1 (Figure 2b).

Supplemental Figure S1: TAIL-PCR product sequences.

> TAIL-PCR product of 772 bp obtained at the 3' end of the resistance cassette of AO1 mutant. The sequence contains 273 bp of the 3' end of *APHVII* (black) and 459 bp of MENC catalytic domain of *PHYLLO* gene (grey).

tcttttggcgccgGACCGCCCCGGCGCCTGATAAGGATCCCCGCTCCGTGTAAATGGAGGCGCTCGTTGATCTGAGCCTTGCCCCCTGACGGAC
GGCGGTGGATGGGAGATACTGCTCTCAAGTGCTGAAGCGGTAGCTTAGCTCCCCGTTTCGTGCTGATCAGTCTTTTTCAACACGTAAAAAGCGG
AGGAGTTTTGCAATTTTGTTGGTTGTAACGATCCTCCGTTGATTTTGGCCTCTTTCTCCATGGGCGGGCTGGGCGTATTTGAAGCGGGTACCGG
GCCCGTCATCCCATGGAAGCTTCATTGATGCGCACCAGTTGCGGCGGCGGGGTCGCAGCGGAACTTGAGGAGGAGGAGGTTGAGGGAGGCGGTG
CGAGTAGGTCGGTGACGGAGGTGTGGAGCGAGGCCGCCAGCGCTGACAGCAGCGCGCTCTCCAGGCCGAACCTGAGGAGTGAGGGCGGCAGCAG
CGTTGCAGCAGCAGCGGCGGGAAGTGGACAGTGCGAGGAGGCGGGCCCATGGGAGACTTGTTGCATTGCACTCCGGTCCTTGTGAGGTGCTCCC
GCGAGCCCCCCAACCGCCTGATTGCACCCAACCATCAACAGCATCCCCGCACTAGCTCCTCCGCAGCATGACCCATCACCGCAGCAGTCCCCCA
CACCCCACACTCCACACACGCCGCACACCCCCACGCCCCACAACCCCACAACCCCACACGCCCCACACCCACATCTCCACGCCCCAAACGCCCC
CACACCCCACATctatacaa

> TAIL-PCR product of 868 bp obtained at the 3' end of the resistance cassette of AS1 mutant. The sequence contains 101 bp of the 3' end of *APHVII* (blue) and 693 bp of *MENB* gene (grey).

ccttaGCGCGGACCGCCCCGGCGCCTGATAAGGATCCCCGCTCCGTGTAAACGGAGGCGCTCGTTGATCTGAGCCTTGCCCCCTGACGAACGGC
GGTGGATGGAAGATACTGCTCTCAAGTGCTGAAGCACCCGGAAGAGGCGCCCCCTTAGCCATGGGTGCACGGTGCCGTCAGTCGCGCCCCGGCG
ATGTGGCGCCGCGTGGCCAGCCTGGGCAAGGAGGAGCTGACAGACGTCATCTATGAGAAGTCGGAGGAGGGCATTGCCAAGGTGGGCGTGGGGG
TAGGGCTCACGACGCGCATGGGGCCGGGTTTGCCCCTGCTGAGTTGGTCACACCTGAAATGTGGGTGCACGTGTAACTGCTGGGACACCATTGT
GATGGTGCATCTGTCGCATCAAGCCTACTTCCGCCACGTCTGTTGAAGCAGGCCCAGGCGCACAAGCCTGGCCAAACATGCAAACTGCTAACCA
TTTGCCAACCCCTTGAACAACCACCCAGATCACCATCAACCGGCCCGACAAGCGCAACGCCTTCCGGCCACAAACCAGTAAGCACCCCGGGGTC
CGGGGCACGTGGCGATGGACGTGTACGTGTGTGTGTGTGTGTGTGCGCGCGCGCATGTGTGTGTGTGTGCGTGCGTGTGTGTGTGTGTGT
GTGTGTGTGTGTGTGTGTGTGTGTGTAAAAAATCTTtatatttatttaacaaagcacgcgcgcggggacagagacactccgcgtgtgtgagggg
ggggcgcacacacactctgtgtgtgtcacgcgtagctgtgtgacatatccccccccccccaccgcgtgtgtgtgtgtgtgtgtgtgtgtgtgtgc
gcgagaaaaaaaaaaaaaatta

> TAIL-PCR product of 753 bp obtained at the 3' end of the resistance cassette of AS2 mutant. The sequence contains 273 bp of the 3' end of *APHVII* (blue) and 392 bp of *HEL22* gene (grey).

tcttaGGCGCGGACGCCCCGGCGCCTGATAAGGATCCCCGCTCCGTGTAAATGGAGGCGCTCGTTGATCTGAGCCTTGCCCCCTGACGAACGGC
GGTGGATGGAAGATACTGCTCTCAAGTGCTGAAGCGGTAGCTTAGCTCCCCGTTTCGTGCTGATCAGTCTTTTTCAACACGTAAAAAGCGGAGG
AGTTTTGCAATTTTGTTGGTTGTAACGATCCTCCGTTGATTTTGGCCTCTTTCTCCATGGGCGGGCTGGGCGTATTTGAAGCGGGTACCGGGCC
CGTCATCCCATGGAAGCTTAAAGGAGTCGTTCTCCAGATGGTGACCACAGACCACTTCTCAGTGGCCCCTGGCTGCCTGCGCCGCCACCCCCGC
CTTGGCTGCCCCAGCCGCCTCCACCTCCTGCACCACCTGTACCTCCCTGCGGCCCCCAGCCGTCCCCGCCGTCCCCTCCTTCTCCACCATGGCC
GCCTGGACCAGCCTTAACCAGAGCCGAGCCGCCGCCGCCCCCTGGCGCGAAAGCAGGCGGCACGTAGCCCCTCGCGCTGGGGCCCGGGCCCGCC
CCTGACGGCCCCTGCTGCCCCTGGTGTGGAGCGCCGTAGCCCCCATAGCCTCCGAGGGCTTGTTGCTGCCCCTGCTGCTGCTGCCCCTGCTGCT
GCTGCTGCTGCTGTTGCCCCTGCTGTTGCTGTTGCCAAGACAGTCCCCCGGCCGCAAAGCCGCCGCCCGCGTTACCACACTGGGGcaaaaactt
a

> TAIL-PCR product of 793 bp obtained at the 5' end of the resistance cassette of AS2 mutant. The sequence contains 708 bp of *MENA* gene (grey).

tatctgCAGGTGTGACTGAACGAAGAGGAGAGGCGCCCCCTTAGCGGAGTGCGATATCAAGCTTCTTTCTTATCCTTCGCGTGCGTCGCTCCAG
CAAGCAGTAGTATCACCATACGCGGCGCAAAGATGCCCAATTGCACGTATGGCGCTGAGGCGCGCGTCGGCCTTCCCCGGGCCGCATCCGAGCG
GCCGGTTTCTGACGCCGCTGCAGTCTGCATCGGCCAATGCGTCCAGTCTAGTGATTGAGTTGCAACCGCAATTCAAGCAGGAGGCATCGGAGGC
AGATGTCGTCGTGGAGACTGGCGCAGTGCTTGCACCCAGCGCAGAGCCCGCGACATCCGCGCCAGCGCCCAGCGAGTCGTCTCAGCAGCCGGGG
GCGGCAGCACAACCCTCAGTTGCAGTTCCGTTTGAAACGGACAAGAAGAAGCTGTGGCTGGCTGCCATCAAGCCCCCGATGTACTCGGTGGGCT
TCATGCCCGTGCTGGTGAGTGCTACTCGCGCTGCTAGCTGGGCCGACAGAGGCGGACAAATACACCCATGTGGTGGTGTCGTGGGGTCATGTTG
TTGGGGGCGTGCTCCAAACGATGGTTGGGCCTGCGTGGGACCCGCGCGGTGTTCCTTTGGTTTGGGCGTGCCATGTACGGACCAAACCAACAAT
CGAAATCGCACTAGGCCGGCTGCATCTATGCATCCACCGTCCAGCTGGCCTCAATCCGCGGACACTCCCAAACCCTTCATCTTGCACACACCCA
AACTTCCcaaaacacgcacccgccgcacacaaaaattctaa

> TAIL-PCR product of 1350 bp obtained at the 3' end of the resistance cassette of 25.1 mutant. The sequence contains 259 bp of the 3' end of *APHVIII* (blue) and 535 bp of *MENE* gene (grey).

gggtgtatagtgtggacgttggGATCCCCGCTCCGTGTAATGGAGGCGCTCGTTGATCTGAGCCCTGCCGCCTGACGAACGGGGGTGGATGGAA
GATACTGCTCTCAAGTGCTGAAGCGGTAGCTTAGCTCCCCGTTTCGTGCTGATCAGTCTTTTTCAACACGTAAAAAGCGGAGGAGTTTTGCAAT
TTTGTTGGTTGTAACGATCCTCCGTTGATTTTGGCCTCTTTCTCCATGGGCGGGCTGGGCGTATTTGAAGCGGGTACCCTGGCTGCCAGTTGCT
GGGCACCAGTGGTCAATAAGGCACAAAGGCGGCACCGTTTTTGCTGCCGTAGCATGATAAGGGCCATTGCTGCCGGAGTGCTGCTCTTGTGGCT
GACGCTGCACCTGCAGGTCACGGCCAGCCTCTGCCACGGCCTGCTGCGGGAGGCCTGCGCATGTGACGTCGTGAAGAACCACCGCCGGCGACAG
CCGCTGGAGtgcctccgccagctcagccacgctccagcgccagtttacggggcagaggaggcagccggtatcgaggcacgccagcatggcttcg
atcatgacagcgctggtctgcgcgatcagaaccaccatcgagccgactggggctagcgggcgctgcaacccgcccaccccgcaagccgatagcg
cgcgggtgatcagcgcgatgcgatgcacaaactcccacctggtgacagagcgtcgggtggaagctgcttcgtctgcacgagtgggatggccccc
accgccaataaacaacggagctgtaatgctcggtgccgatggaccccaagcgccatgaaaccttgtcaagacgcacctcatatcgtatggatat
ctcctatccagcaagagggacgtccaaccggtgggagccgagctgaaactcgatttgtgccaacctctgcattcaacgctccgaccatagcaat
aaaatgacaagataaacctccgatttttctgtcattgtgtctatataccccgaaatccgatccctagactgaaatcctctccgataccccacaa
atcccccattgggggcttatacctccgctttctccctttttccccccaccccacacgcccaattccagttcaaggccccacgtcaccgccaacaac
ttcccgcccagcagtggcgcgggcagcgagtaaggaccgtgggttcgggagacggcctctactcgctttcccactccctggataacgggtctag
gccgtgtcctcgaatccggccgacggattctgtactcgattacagtattgtgatctggtatgctaccccgcggacccctgctccctctgttcgc
ctgattatgttttcctctcccatcttctccgcct

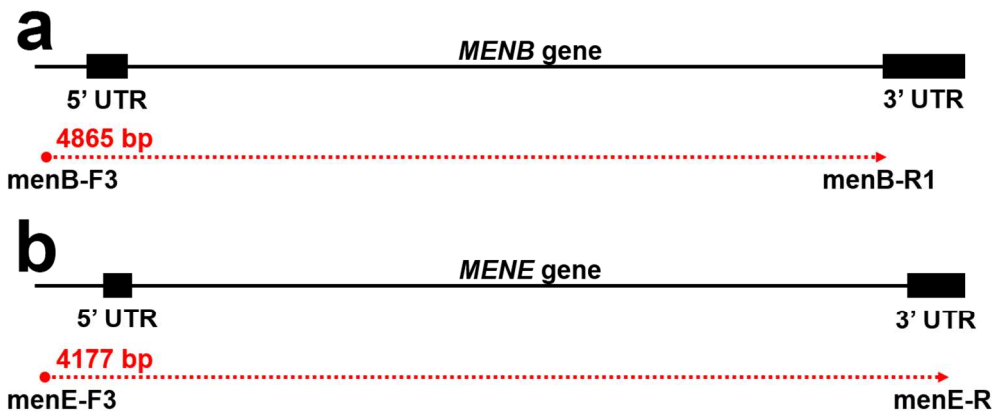

Supplemental Figure S2: Amplification of MENB and MENE genes and their flanking regions. (a) MENB gene PCR product (4,865 bp) amplified by menB-F3/menB-R1primers covers the MENB gene from 467 bp upstream of the ATG codon to the STOP codon. (b) MENE gene PCR product (4,177 bp) amplified by menE-F3/menE-R primers covers the MENE gene from 403 bp upstream of the ATG codon to 174 bp after the STOP codon.

Figure S2
117x49mm (300 x 300 DPI)

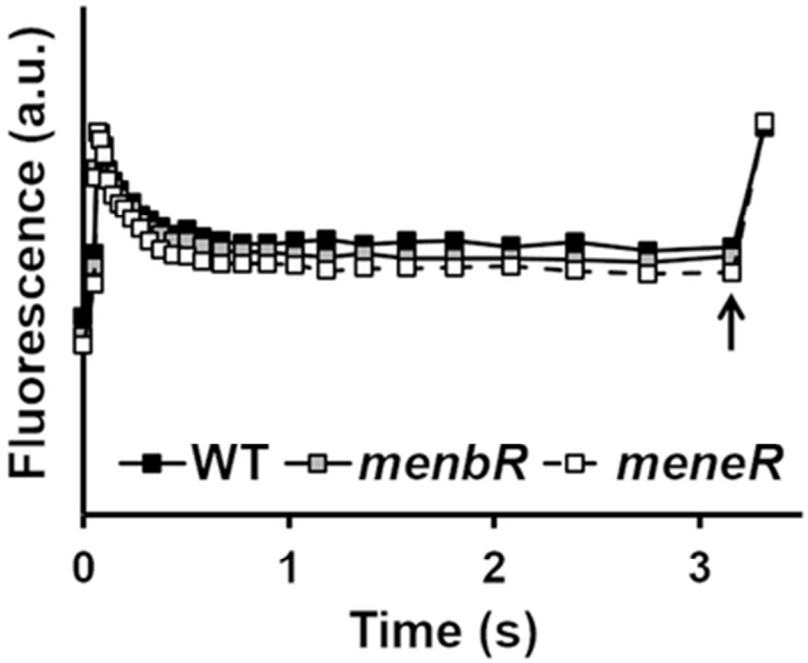

Supplemental Figure S3: Chlorophyll fluorescence induction curves of wild-type and complemented strains. Chlorophyll fluorescence induction curves upon illumination at ~ 110 µmol photons (λ = 520 nm) m-2 s-1 of C. reinhardtii wild-type and complemented strains (menbR, meneR) after acclimation to dark anoxic conditions (>12 h). Arrows indicate the time when the saturating light pulse was given.

Figure S3
34x29mm (300 x 300 DPI)

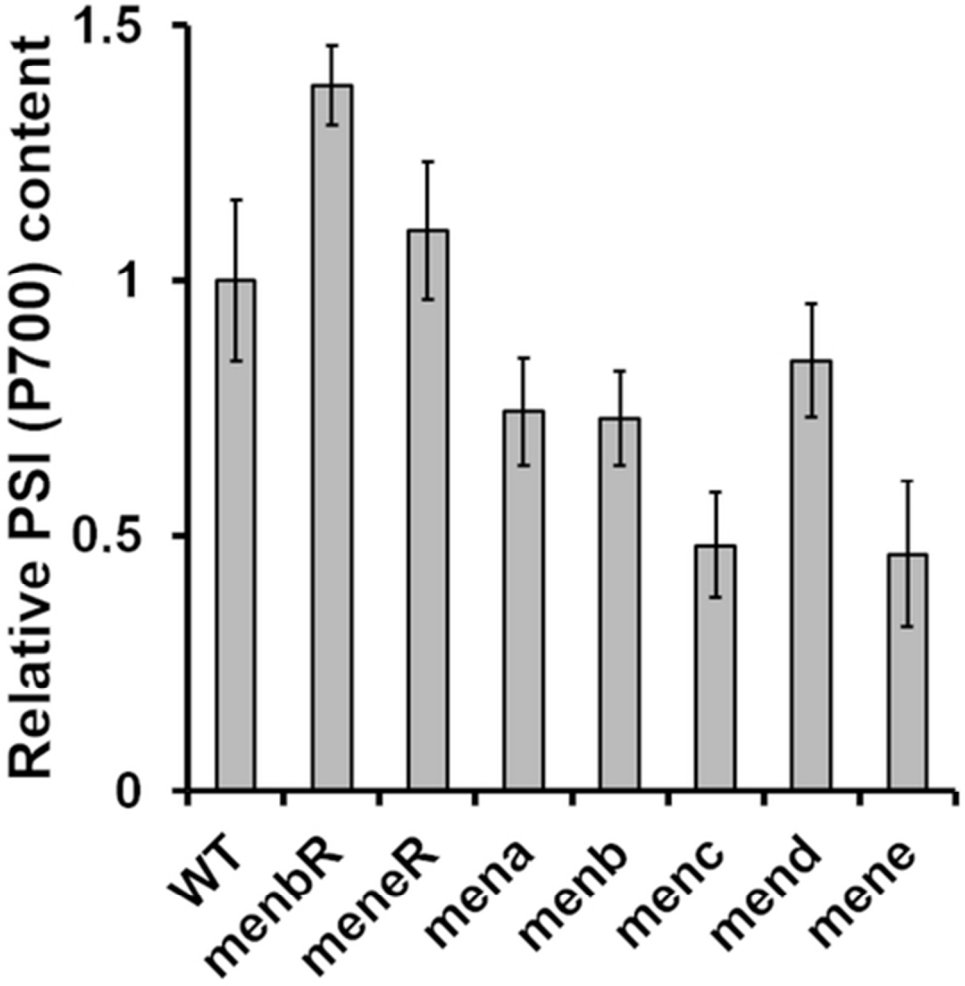

Supplemental Figure S4: PSI relative content.
PSI relative content (wild-type value normalized to 1) determined from the maximum absorption changes at 705-740 nm between dark acclimated cells (P700 oxidized) and cells exposed to saturating light in the presence of DCMU (20 µM) (P700 reduced). Values are the average of three independent experiments.

Figure S4
45x47mm (300 x 300 DPI)

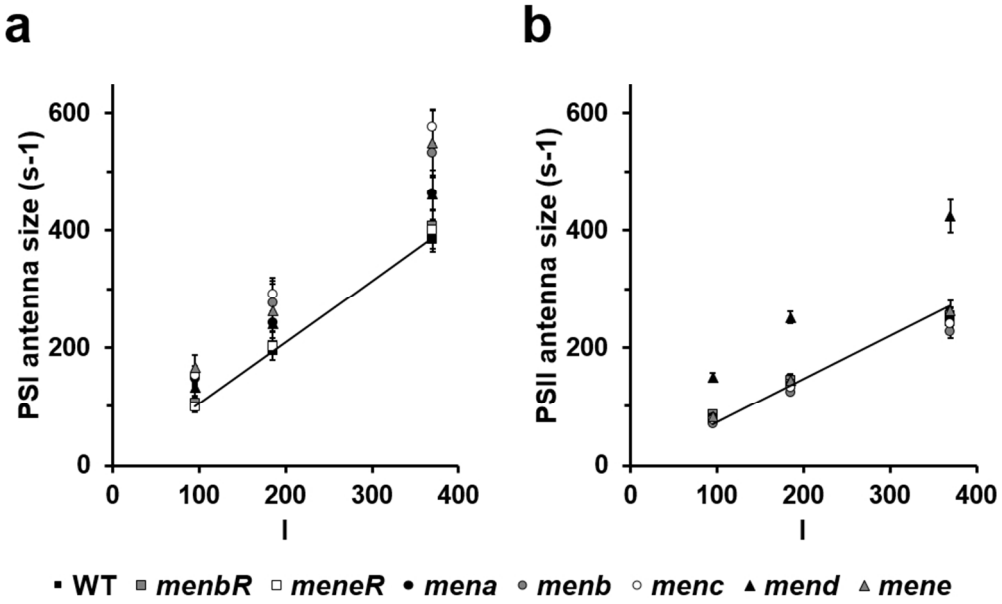

Supplemental Figure S5: Determination of PSI and PSII antenna size in wild-type, complemented and men mutant strains.
(a) PSI antenna size estimated from ECS absorbance transients (520-546 nm) in DCMU (20 µM) + hydroxylamine (1 mM) - poisoned cells as a function of light intensity. The initial rate of this signal is proportional to the antenna size of PSI (s-1). (b) PSII antenna size estimated from chlorophyll fluorescence transients in DCMU (20 µM) - poisoned cells as a function of light intensity. The mid-rise time of this signal is proportional to the antenna size of PSII (s-1). Values are the average of three independent experiments. Values reported in Figure 5g are the values of the slopes, normalized on the value of the slope for wild type.

Figure S5
85x54mm (300 x 300 DPI)

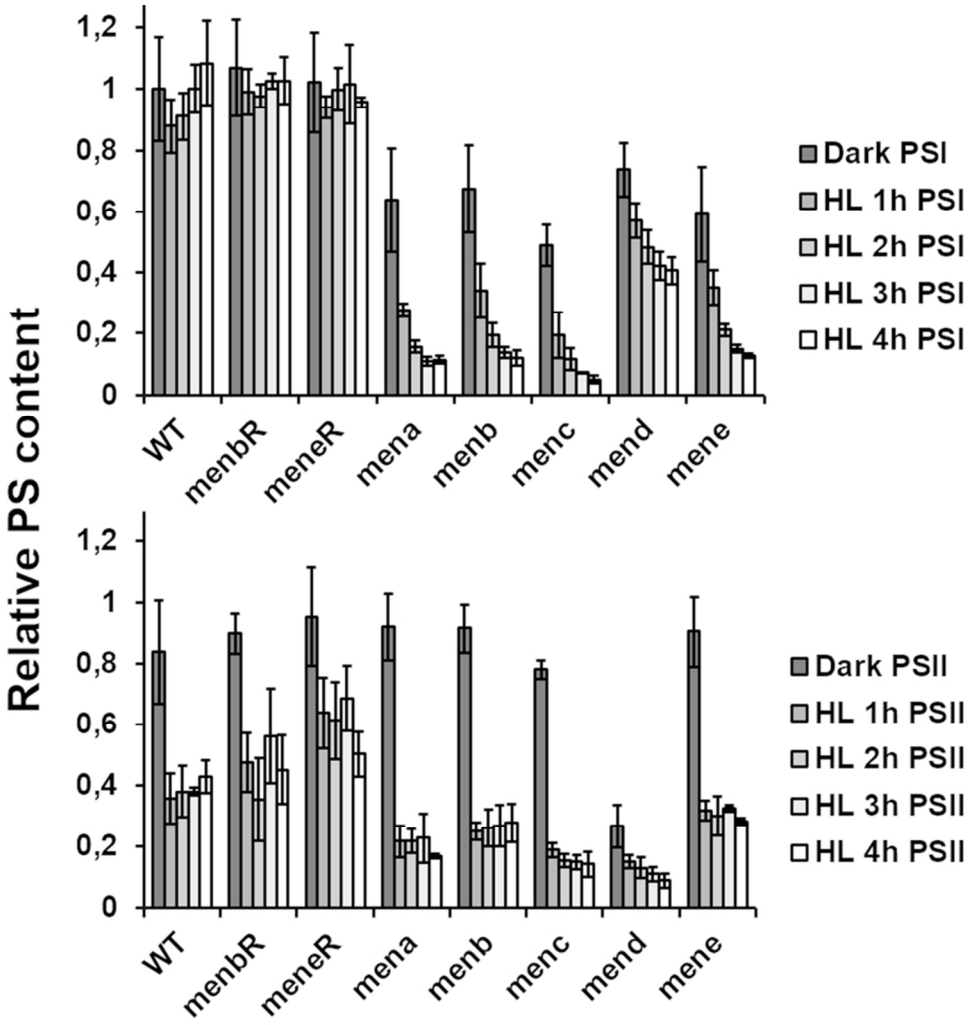

Supplemental Figure S6: PSI and PSII content in control and mutant strains.
ECS measurements (520-546 nm) on cells grown in low light and then transferred for four hours at high light intensity (HL, 400 µmol photons m-2 s-1). Active PSI center content of wild-type cells adapted to darkness was normalized to 1. Values are the average of three independent experiments.

Figure S6
79x81mm (300 x 300 DPI)

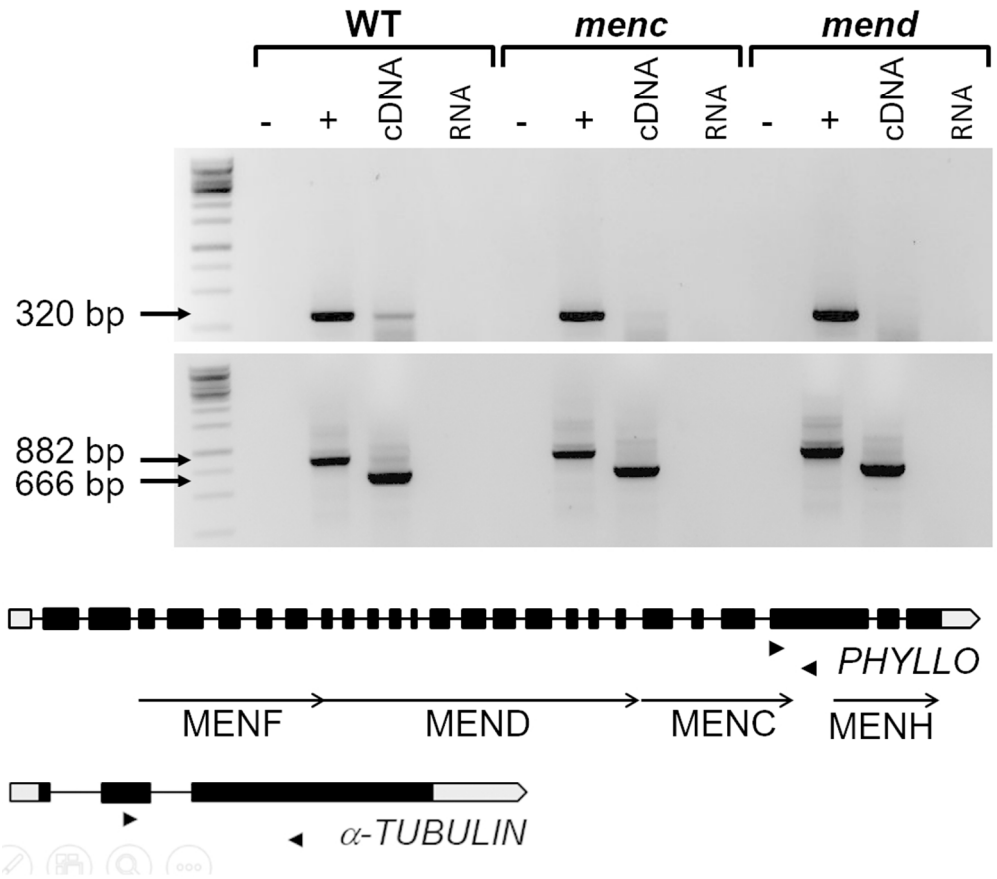

Supplemental Figure S7: RT-PCR analysis of menc and mend mutants.
Upper, RT-PCR analysis using primers binding PHYLLO (size: 330 bp) and β-tubulin (size: 666 bp) cDNAs. PCRs were performed on samples without nucleic acid (-, negative control); on DNA (+, positive control), on cDNA and on RNA treated with Dnase (negative control). Lower, organization and structure of Chlamydomonas alpha-tubulin and PHYLLO genes. Exons are indicated by black boxes. The positions of the PHYLLO-F2 and PHYLLO-R2 primers (Table S2) used to produce and amplify PHYLLO cDNA are indicated. Analyses were performed according to standard protocols using M-MLV Reverse Transcriptase (Promega). P1Tub and P2Tub (Table S2) were used to produce and amplify alpha-tubulin cDNA.

Figure S2
93x82mm (300 x 300 DPI)

Supplemental Figure S8: Sequence alignment of PHYLLO protein from *C. reinhardtii* (CrPHYLLO) and *A. thaliana* (AtPHYLLO) with *E. coli* MenF, MenD, MenC and MenH proteins (EcMenF, -D, -C, -H).

The PHYLLO locus found in plants and algae comprises the four Men modules responsible for the first four enzymatic steps of menaquinone biosynthesis in bacteria. In *A. thaliana*, the C-terminal chorismate binding domain is truncated from the PHYLLO MenF module unlike *C. reinhardtii* in which MenF structural integrity was maintained. The protein sequences were aligned using Clustal Omega and BoxShade.

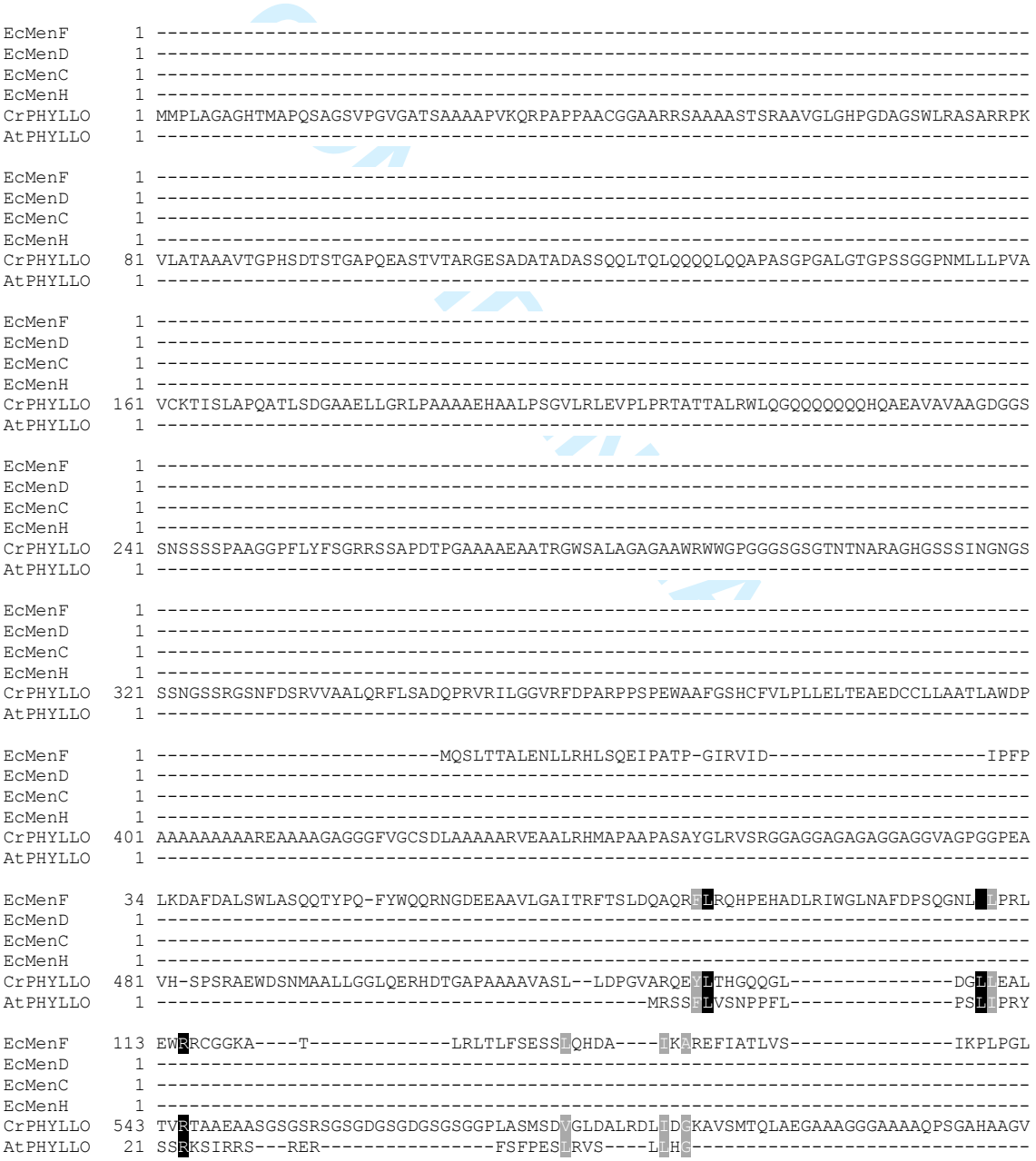

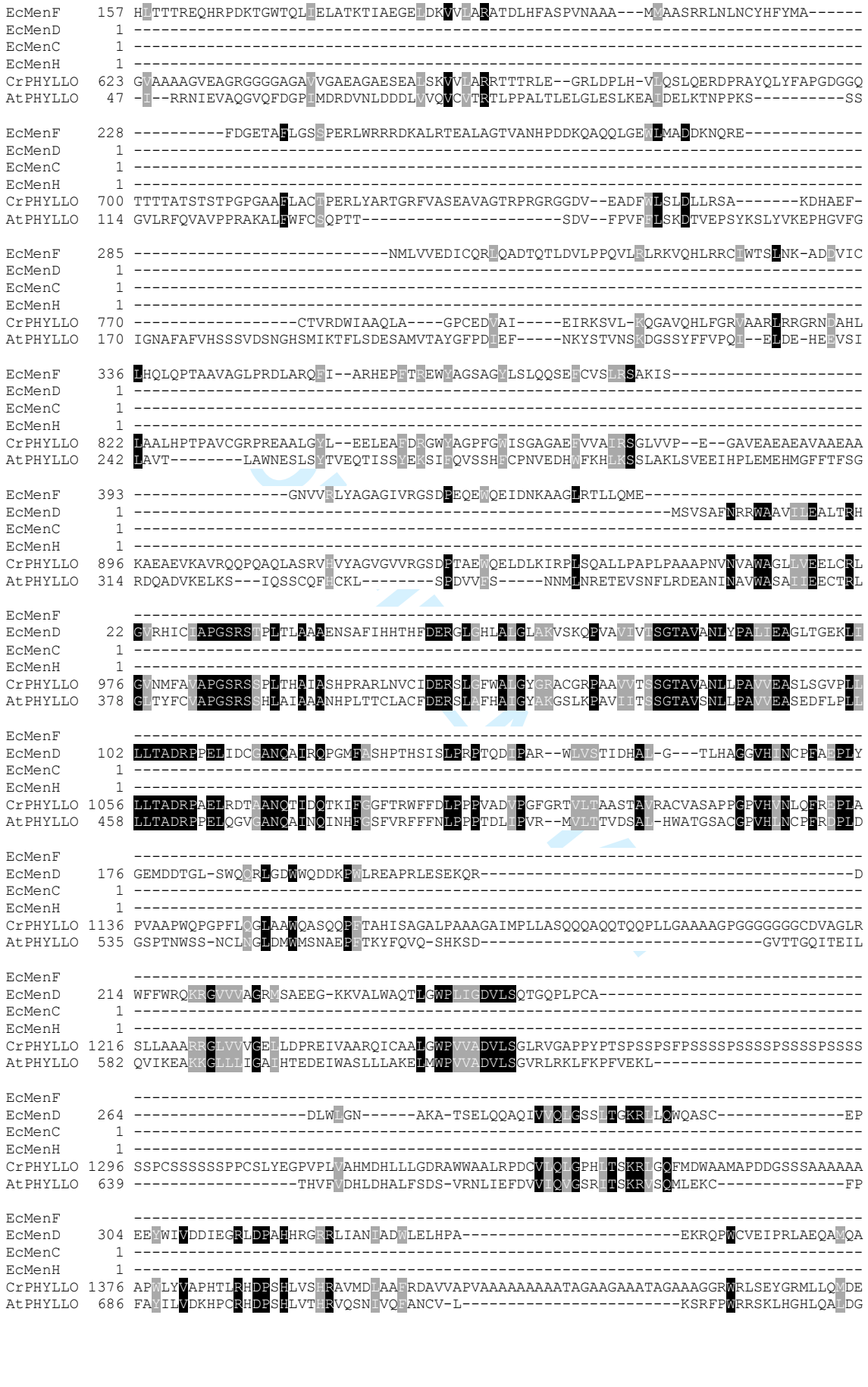

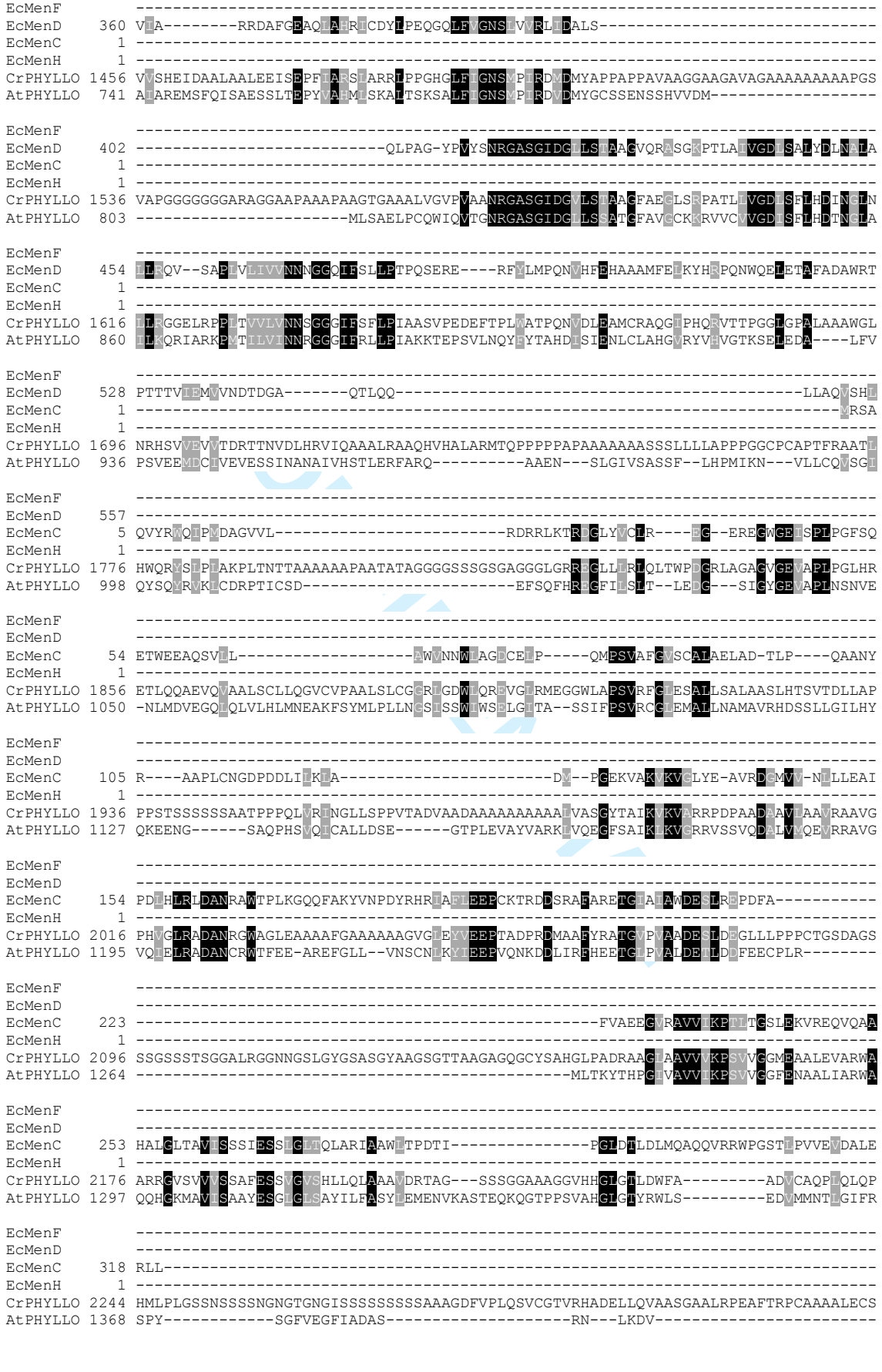

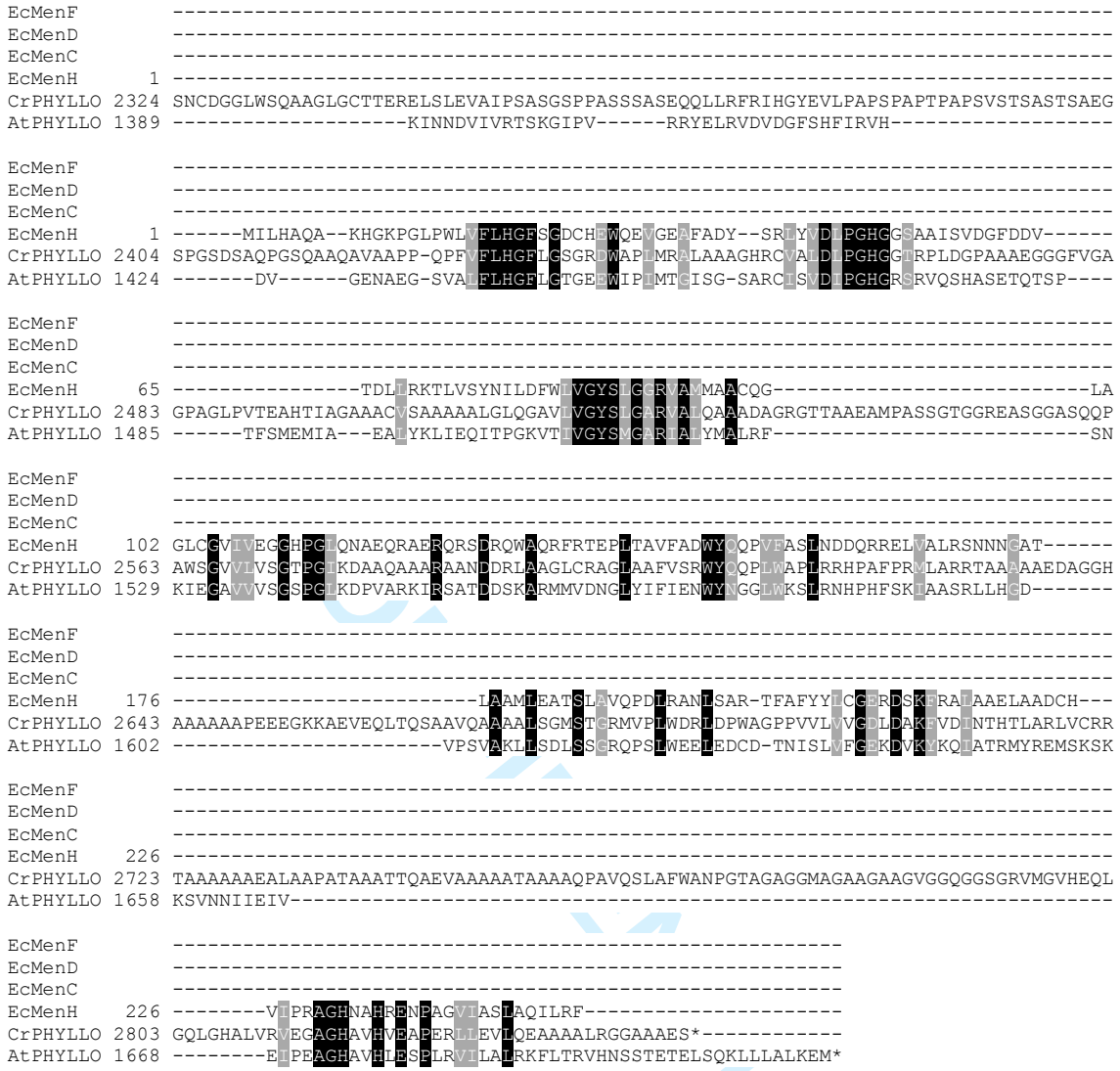
EcMenF
EcMenD
EcMenC
EcMenH 1
CrPHYLLO 2324 SNCDGGLWSQAAGLGCTTERELSLEVAIPSASGSPPASSSASEQQLLRFRIHGYEVLPAPSPAPTPAPSVSTSASTSAEG
AtPHYLLO 1389 KINNDVIVRTSKGIPV RRYELRVDVDGFSHFIRVH
EcMenH 1 MILHAQA KHGKPGLPWL FLHGF SGDCH WQE GE FADY SR YVDL PGHGG AAISVDGFDDV
CrPHYLLO 2404 SPGSDSAQPGSQAAQAVAAPP-QPF FLHGF LGSGR WAP MR LAAAGHRC ALDL PGHGG RPLDGPAAAEGGGFVGA
AtPHYLLO 1424 DV GENAEG-SVA FLHGF LGTGE WIP MT ISG-SARC SVDI PGHGR RVQSHASETQTSP
EcMenH 65 TDL RKTLVSYNILDFW VGYS GGR A MAA CQG LA
CrPHYLLO 2483 GPAGLPVTEAHTIAGAAAC SAAAAALGLQGAV VGYS GAR A QAA ADAGRGTTAAEAMPASSGTGGREASGGASQQP
AtPHYLLO 1485 TFSMEMIA EA YKLIEQITPGKVT VGYS GAR A YMA LRF SN
EcMenH 102 GLC GV V EG HPG QNAEQRAE RQRS DRQW QRFRTEP TAVFAD WY QQP E AS NDDQRREL ALRSNNN AT
CrPHYLLO 2563 AWS GV VL VS TPG KDAAQAAA AANDDRL AAGLCRAG AAFVSR WY QQP W AP RRHPAFPR LARRTAA AAEDAGGH
AtPHYLLO 1529 KIE GA VV VS SPG KDPVARKI SATDDSK RMMVDNG YIFIEN WY GG W KS RNHPHFSK AASRLLH D
EcMenH 176 LAAM EATS V QPD RAN SAR-TFAFYY C RDSK RA AAELAADCH
CrPHYLLO 2643 AAAAAAPEEEGKKAEVEQLTQSAAVQA AAA SGMST RMVP W DRL DPWAGPPVVL V GDL DAK VD NTHTLARLVCRR
AtPHYLLO 1602 VPSV AKL SDL SS RQPS W EE EDCD-TNISL F K DV K KQ ATRMYREMSKSK
EcMenH 226 TAAAAAAEALAAPATAAATTQAEVAAAAATAAAAQPAVQSLAFWANPGTAGAGGMAGAAGAAGVGGQGGSGRVMGVHEQL
AtPHYLLO 1658 KSVNNIIEIV
EcMenH 226 V PRAGH NA REN PAG VIAS AQILRF
CrPHYLLO 2803 GQLGHALVR EGAGH AVH VEA ER LEVL QEAAAALRGGAAAES*
AtPHYLLO 1668 E PEAGH AVH ES PLR VI LA RKFLTRVHNSSTETELSQKLLLALKEM*

Supplemental Figure S9: Sequence alignment of CYP25 protein from *C. reinhardtii* (CrCYP25) with its two homologs in humans (HsCYP4F2 and CYP4F11).
The protein sequences were aligned using Clustal Omega and BoxShade.

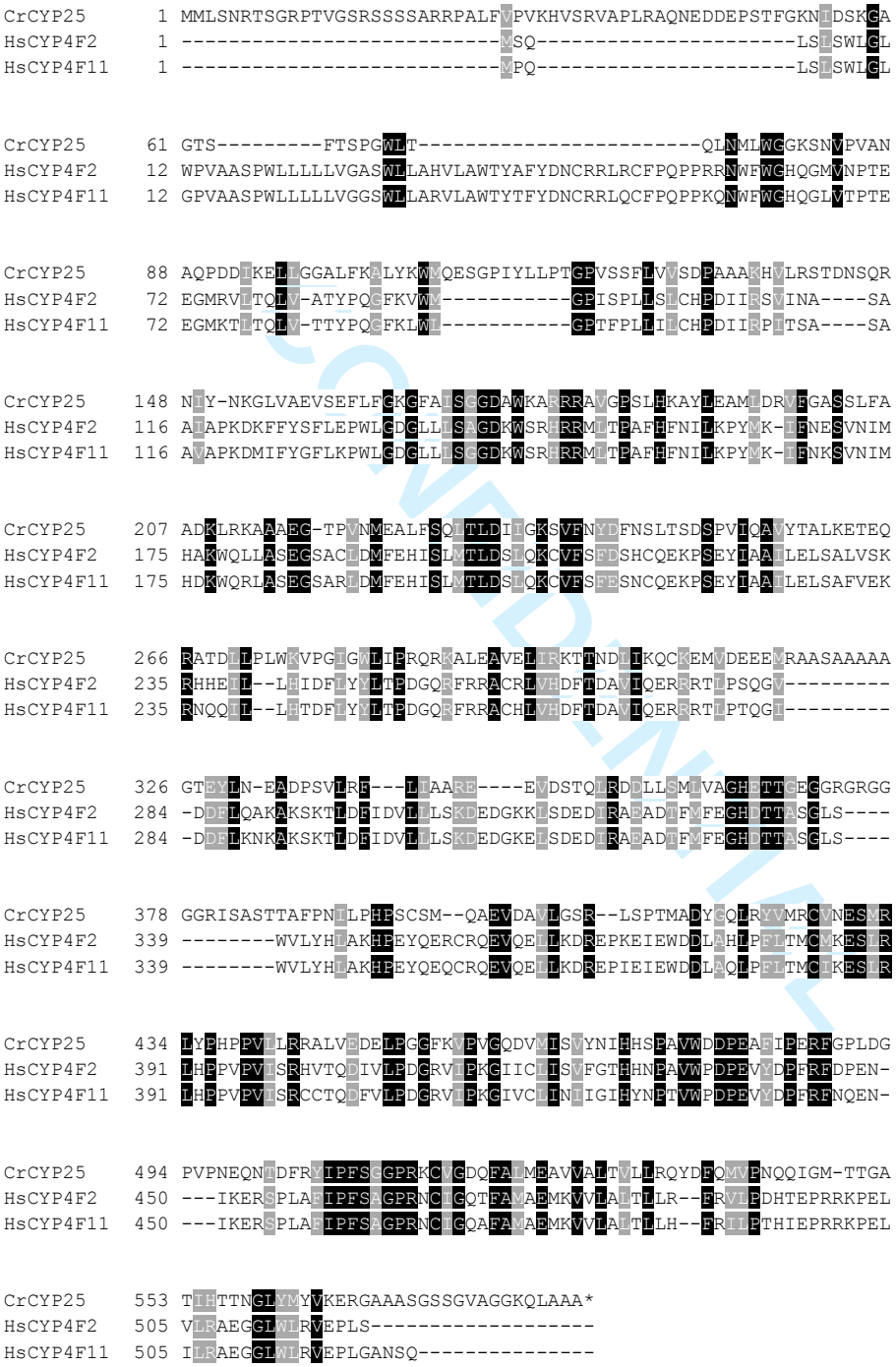

Table S1: Cosegregation analysis of the antibiotic resistance cassette with the fluorescence phenotype.

Fluorescence phenotype[a]	Mutant		Wild type	
Antibiotic resistance[b]	+	-	+	-
Strains	% of meiotic clones[c]			
AL2	10.1	13.7	6.5	69.7
AO1	48.3	0	0	51.7
AO2	0.5	2.8	1.1	95.6
AS1	40.5	0	0	59.4
AS2	50.5	0	0	49.5
24.1	41.9	12.5	36.8	8.8
25.1	51.5	0	0	48.5

[a]The fluorescence phenotype in anoxia was determined as described for Figure 1. [b]Antibiotic resistance: + and – indicate resistance or sensitivity to hygromycin (AL2, AO1, AO2, AS1, AS2) or paromomycin (24.1, 25.1), respectively. [c]Results are expressed as a percentage of independent meiotic clones (150-300 clones analyzed for each cross).

Table S2:

Table S2 : Primers sequences (5'→3')

Primer	**Sequence** (5'→3')
APH7-F	TCGATATCAAGCTTCTTTCTTGC
APH7-R	AAGCTTCCATGGGATGACG
APH7-R2	AGTTCCTCCGGATCGGTGAAG
APH7-R3	AGAATTCCTGGTCGTTCCGCAG
APH7-R4	TAGGAATCATCCGAATCAATACG
APH7-R5	CGGTCGAGAAGTAACAGGG
APH8-F	TCAGGCAGACGGGCAGGTG
APH8-R	CTGGGTACCCGCTTCAAATA
HygTail2	ACCAACATCTTCGTGGACCT
HygTerm1	CGCGAACTGCTCGCCTTCACCT
HygTerm2	TCGAGGAGACCCCGCTGGATC
HygTerm3	CGATCCGGAGGAACTGGCGCA
menB-F3	AACATGCCGCAGCTATTCTC
menB-R1	TCAGGGCAGGCGCTTGAACTTG
menE-F3	TTGAACAGTGCAGCCGTTAG
menE-R	CCGGCTACACTTCCTCCTTC
pAPH-8F	GCGGGAGTTGTTTGTCAAGG
pAPH-8R	GACTGCGATCGAACGGACAC
ParoTerm2	TTGGTGGCTGGGTAGGGTTG
ParoTermB	GATGGGGCGGTATCGGAGGA
ParoTermC/1	CGGCTGTTGGACGAGTTCTTCTG
PHYLLO-F2	GAATGGAGGCGGCGTTAGAG
PHYLLO-R2	TGCTGCTGCTGCTGCTAATG
P1Tub	AACACCTTCTTCTCGGAGAC
P2Tub	GAGCTGAGCATGAAGTGGAT